Quantitative Assessments of Staphylococcal Phage and Biofilm Properties for Evaluating Phage as Antibiofilm Therapeutics

A Thesis submitted to the Faculty of the Worcester Polytechnic Institute in partial fulfillment of the requirements for the Degree of Master of Science in Chemical Engineering

---

Submitted by:

_____

Kim Mori

Approved by:

_____

Elizabeth J. Stewart, Ph.D.
Assistant Professor, Department of Chemical Engineering

_____

Eric M. Young, Ph.D.
Assistant Professor, Department of Chemical Engineering

_____

Christina M. Bailey-Hytholt, Ph.D.
Assistant Professor, Department of Chemical Engineering

Abstract

Due to the difficulty of treating *Staphylococcus epidermidis* biofilm infections with traditional antibiotics, lytic phage are emerging as potential antibiofilm therapeutics. *S. epidermidis* frequently causes biofilm infections on medical devices and is estimated to be responsible for 50-70% of infections associated with surgical implants. This thesis studies the effect of phage Andhra, a lytic staphylococcal phage, on *S. epidermidis* biofilms to assess how different ratios of the concentrations of phage to bacterial cells in the biofilm affect biofilm height, porosity, and biomass. Phage Andhra was found to have a size of 121.36 ± 1.47 nm in diameter and a zeta potential of -12 ± 0.58 mV. A quantitative method to assess the bacterial cell concentration in biofilms prior to phage addition was developed where the local number density of bacterial cells and the total biofilm biomass extracted from image analysis of confocal laser scanning microscopy image volumes collected at two different length scales were used to estimate the number of bacterial cells in the biofilm. The development of this quantitative method for determining the ratios of phage to bacterial cells in the biofilm upon the addition of phage to biofilms allows for a more controlled method for studying phage treatments. With the known concentrations of phage and bacterial cells in the biofilm, the ratio of these concentrations—the multiplicity of infection (MOI)—was varied to study how the gross structure of the biofilm changes with MOIs of 0.07, 0.67, and 1.16. Overall, there is not a linear relationship between the increasing value of the MOI and the height, porosity, and biomass of the biofilm. The height and biomass decrease from MOIs 0 to 0.07 and 0.07 to 0.67 and then increase from an MOI of 0.67 to an MOI of 1.16. The porosity decreases at an MOI of 0.67 and increases at an MOI of 1.16. Although there were some significant changes in the biofilm properties of these experiments, most changes in properties were modest across MOI values used. Characterization of the size and zeta potential of phage Andhra, the development of a controlled method to calculate MOI prior to phage addition to biofilms, and studying the effects different MOIs have on biofilm structure are critical steps toward evaluating lytic phage Andhra as a biofilm therapeutic. Moving forward, additional factors that must be considered when evaluating phage treatments include the viability of bacterial cells within the biofilm, the penetration of the phage within the biofilm, the interactions of the phage with the biofilm matrix, and the different time points and dosages of phage treatments. This M.S. thesis made important steps to provide new insights into the potential of lytic staphylococcal phage as therapeutics for biofilm infections.

Acknowledgements

This research was completed using the facilities provided by Worcester Polytechnic Institute's Department of Chemical Engineering. I would like to thank all the people who have helped and guided me towards success in completing my research at WPI.

First, I would like to thank my advisor Professor Elizabeth Stewart for proposing this topic and providing all the guidance and knowledge I would need to succeed. I would like to thank her for being patient and understanding when it seemed like I was being thrown with many obstacles and roadblocks imaginable.

Next, I would like to thank all those in the Stewart Lab. Without the help from Patryck Michalik and Lily Gaudreau on understanding the basic concepts in the lab and image analysis, I would not have been able to successfully analyze and understand the data I collected. I would also like to thank Sydney Packard for being my mentor from day one and helping me acclimate to the lab environment. She supported me by teaching me how to successfully run experiments and understand the material I was working with in a critical lens.

In addition, I am grateful to Dr. Asma Hatoum-Aslan, University of Illinois Urbana-Champaign, for helping the Stewart lab acclimate to working with phage for the first time in our lab. Her phage amplification and titering protocols were instrumental to this project.

Many thanks to Professor Christina Bailey-Hytholt and Professor Eric Young for being a part of my committee and providing helpful and constructive feedback.

Lastly, I would like to extend my sincere thanks to my friends and family for showing me constant support and encouragement while working on completing my research.

Table of Contents

Table of Figures

Table of Tables

Table of Equations

Introduction

Staphylococcal epidermidis is a significant pathogen that plays a vital role in biofilm infections. As a common cause of nosocomial infections, *S. epidermidis* can colonize the surfaces of medical implants and devices, leading to biofilm formation that can cause severe infections (Otto, 2009). In fact, *S. epidermidis* infections are responsible for 50-70% of all infections associated with surgical implants (Xu & Siedlecki, 2022). The ability of *S. epidermidis* to form biofilms on medical device surfaces presents a significant challenge to treat these infections. Biofilms are difficult to treat with antibiotics due to the majority of bacterial cells in biofilms being metabolically inactive, or not actively growing. Since antibiotics target metabolically active bacterial cells, antibiotic treatments are not as effective on biofilms as on planktonic cells. In addition to antibiotics, alternative therapeutic treatments will become necessary to treat these biofilm infections in the future (Hall-Stoodley et al., 2004).

Bacteriophage, also known as phage, are viral particles that replicate within bacterial host cells. Lytic phage are a type of phage that release viral phage particles over short intervals of time, causing the lethal disruption of the bacterial host cells (Hobbs & Abedon, 2016). Lytic phage are emerging as a promising alternative to antibiotics (Cater et al., 2017). An advantage of lytic phage is that they leave beneficial microbes unharmed while still attacking the bacterial pathogens that are deemed harmful. Lytic phage treatments of biofilms have shown that they can either increase or decrease the biofilm's height, porosity, and biomass by infecting the bacterial cells in the biofilm, being entrapped in the EPS matrix of the biofilm, or being entrapped in the pores of the biofilm (Cater et al., 2017).

Phage therapies are emerging as alternatives to traditional antibiotics. Lytic phage have been widely studied for their effects on biofilm height, porosity, and biomass. However, their ability to treat biofilm infections is not well understood as phage have been reported to interact with biofilms in different ways. The depolymerization capability of the phage enzymes can reduce the biomass in biofilms. By attacking the bacterial cells in the biofilm, phage can decrease the height and biomass in the biofilm. Phage can also interact with the EPS matrix of the biofilm and can become entrapped in the pores of the biofilms, causing the height and biomass to increase (Fanaei Pirlar et al., 2022). The concentration of phage and bacterial cells in the biofilm prior to phage treatment are crucial to determine the effectiveness of phage therapy. However, there is a lack of clarity in determining a controlled method for calculating these concentrations in the literature. The lack of clarity in calculating the concentration of phage and bacterial cells in the biofilm prior to phage treatment is important to address because this can have a great impact on the effectiveness of phage therapy.

The need for analyzing the biofilm structure and defining a controlled method of calculating the bacterial cell concentration prior to phage treatment are crucial topics that have not yet been fully addressed in the literature. Current studies on phage treated biofilms do not clearly define the

concentration, height, and porosity of the biofilm before phage treatment and the biofilm height and porosity is not well defined after phage treatment (Hansen et al., 2019). These studies also do not define a controlled method to analyze how the structure of the biofilm changes upon different concentrations of phage treatment. Moreover, these studies lack a definitive method of calculating the ratio of phage viral particles to the bacterial cells in the biofilm. This can also be described as the ratio of the concentration of phage to the concentration of the bacteria within the biofilm, which is known as the multiplicity of infection (MOI). Some studies have used colony forming unit (cfu) counts to determine the concentration of bacterial cells in the biofilm before and after phage treatment. This method can be inaccurate because of the inconsistency and bias that arises when counting colonies. The number of colonies counted may not represent the actual number of bacterial cells in a sample as multiple bacterial cells clump together to form a single colony, leading to an overestimation of concentration. Some colonies are bigger than others, which might cause the smaller colonies to not be counted, leading to an underestimation of concentration. Additionally, the concentration of bacterial cells in the biofilm changes from the time point of phage addition and the time point after phage addition. Due to the bacterial cell concentration changing in the biofilm, the MOI also changes before and after phage addition and it is not clear about when or how the MOI is determined (Curtin & Donlan, 2006).

The overall goal of my M.S. thesis is to analyze the effects of phage Andhra—a lytic phage that targets *S. epidermidis*—on *S. epidermidis* biofilms to see how different ratios of phage to bacteria concentrations affect biofilm structure. Specifically, my research focuses on studying how three different phage to bacteria ratios (MOIs) influence the change in biofilm height, porosity, and biomass. Studying how the different phage to bacteria ratios influence lytic phage efficacy toward biofilms is important for determining how this affects the biofilm's structure because it will give more insight as to how the biofilm is impacted at a higher concentration of phage versus a lower concentration of phage. Studying the effect phage has on the biofilm at different MOIs brings more understanding to how phage can become a potential therapeutic to treat biofilm infections. My overall goal was achieved through the following objectives:

a. Characterization of the biophysical properties (size, zeta potential, and concentration) of phage Andhra.
b. Development of a quantitative method for controlling initial phage to bacteria ratios in biofilms.
c. Determination of the effect of different phage MOIs on biofilm growth and structure.

Collectively, the work of my thesis shows how the biofilm structure (height, porosity, biomass) is impacted at different phage concentrations in a controlled manner. This research is important for the advancement of phage treatment on biofilms and evaluating the potential of phage becoming a promising alternative to antibiotics.

Background

Bacterial Biofilms

Biofilms are structured communities of bacterial cells that create an extracellular polymer substance (EPS) matrix containing proteins, lipids, polysaccharides, and extracellular DNA (Hall-Stoodley et al., 2004). EPS is the matrix that holds the bacterial cells together in one community. With the help of the EPS matrix, biofilms adhere to different surfaces such as rocks, teeth, catheters, and other surgical implants in the body. Biofilm infections on the body can appear as gum disease, catheter contamination, and implant contamination. The matrix provides the biofilm with the stability it needs to stay intact and connected to a surface (Hall-Stoodley et al., 2004).

Biofilms modify their own structure to increase their survival rate and withstand living in various environmental conditions. Different environmental conditions include mines, rivers, hydrothermal vents, and inactive waters. In different environments, biofilms offer protection to the surfaces they grow on. Biofilms offer protection from UV exposure, metal toxicity, acid exposure, dehydration, salinity, several antibiotics, and antimicrobial agents. The protective qualities come from the self-produced EPS matrix, the pockets of cells formed when the biofilm is in its stationary phase, and the dormant, or metabolically inactive, cells in the biofilm (Hall-Stoodley et al., 2004).

Indwelling medical devices save millions of lives, however, there is always a risk of bacterial biofilm infections growing on medical devices once they are implanted in the body. A bacterial biofilm infection can be treated with antibiotics, but due to the biofilm's protective properties, the antibiotics are not always able to treat bacterial biofilm infections. Although antibiotics may work sometimes, new antimicrobials are needed for the treatment of biofilms (Hall-Stoodley et al., 2004).

Staphylococcus epidermidis

One of the most common nosocomial, or hospital acquired, infections are staphylococcal infections. *S. epidermidis* was not thought of as an opportunistic pathogen, since it naturally grows on the human epithelia, until bacterial biofilm infections were seen using the newly introduced method of electron microscopy in the early 1980s (Hall-Stoodley et al., 2004). *S. epidermidis* bacterial biofilm infections have cost the US around $2 billion annually to treat due to their frequency of occurrence, however most cases do not turn into life-threatening situations (Otto, 2009). *S. epidermidis* biofilm infections are difficult to treat due to their protective EPS matrix and dormant cells in the biofilm. The EPS matrix of *S. epidermidis* consists of polysaccharide intracellular adhesin (PIA), proteins, and extracellular DNA. PIA are β-1,6-linked glycosaminoglycan polysaccharides that allow cell layers to form through cell-to-cell adhesion mechanisms, also making biofilm infections difficult to treat. Biofilms have also become less susceptible to antibiotics due to the presence of dormant cells. Dormant cells are less metabolically active and not actively growing. Therefore, dormant cells do not allow antibiotics to treat these

cells since many antibiotics only target cells that are metabolically active and actively growing. Overall, this is a medical problem and although there are new technological developments being applied to antibiotics, *S. epidermidis* infections are becoming recalcitrant, or not responsive to treatment, to these antibiotics, making it a greater problem the harder it becomes to treat (Hall-Stoodley et al., 2004; Otto, 2009).

Additionally, the different components of the biofilm have different charges. The bacterial cells in the biofilm have a negative charge due to the negatively charged teichoic acids and lipopolysaccharides on the surface of the cell wall. The components of the EPS matrix all have different charges. The PIA of *S. epidermidis* biofilms has a positive charge, which allows the polymer to attach to the bacterial surface in a stable manner (Nguyen et al., 2020). The proteins in the EPS matrix of *S. epidermidis* biofilms, which are usually carboxyl and sulfate groups, are negatively charged. The extracellular DNA in the EPS matrix also has a negative charge (Otto, 2009).

Bacteriophage

Bacteriophage, also known as phage, are the most plentiful replicating organisms on the planet (Hansen et al., 2019). Phage have been present for around a million years and have been constantly evolving (Hansen et al., 2019). The interactions between phage and bacteria have been studied, allowing this field to be constantly expanding to gain more knowledge about the different interactions between phage and bacteria (Hansen et al., 2019). Phages are viruses that infect bacterial hosts as a means of replicating since they are not able to do so without a host.

Phage are composed of a protein capsid, or head, containing genetic material, and a tail that is used for attachment and injection of the phage genome into the host bacterial cell. The phage head is usually either icosahedral or cylindrical in shape. The purpose of the phage head is to protect the phage genome from external factors that could impact the genetic material of the phage. The phage tail is a tubular or helical structure that extends from the phage head. The phage tail is responsible for recognizing and binding to specific receptors on the surface of the host bacterial cell. The tail consists of multiple protein subunits and tail fibers that enclose a central tube. When the phage tail recognizes its specific receptor on the host cell surface, it penetrates the central tube into the cell wall and membrane of the bacterial host cell (Hawkins et al., 2022).

There are two different categories of phage, lytic and lysogenic. Lytic phage replicate by releasing viral phage particles over short intervals of time and causing the lethal disruption of the bacterial host cells upon contact. By infecting the cells, the phage pass on DNA to the bacterial host. In this infection process, the phage particles propagate through cell lysis. During cell lysis, the host bacterial cell wall and membrane are broken down, making it easier for phage to infect new cells. This whole process of phage propagation is known as lytic growth. Lysogenic phage attack the

host bacterial cells by injecting its DNA into the host cell. Lysogenic phage undergo replication as prophages that do not directly result in virion production or release (Marianne Poxleitner, 2018).

The type of phage most used for phage therapeutics are strictly lytic phage due to their host specificity, self-propagation, and easy isolation for pathogens. Lytic phage tend to have a much narrow host range in comparison to lysogenic phage. The specific host range allows for more specific phage therapeutic analyses to ensure that the phage will propagate and infect its targeted host (Hansen et al., 2019).

Staphylococcal Phage

The phage strains that have *S. epidermidis* as its bacterial host are a part of the bacteriophage families of *Siphoviridae, Myoviridae,* and *Podoviridae* (Cerca et al., 2007; Curtin & Donlan, 2006; Fanaei Pirlar et al., 2022; Gutiérrez et al., 2012; Hawkins et al., 2022). Phage Andhra comes from the *Podoviridae* family, which consists of strictly lytic phages. Phage Andhra was discovered through growing *S. epidermidis* RP62A with raw sewage. This coculture was then purified by plating the individual plaques with *S. epidermidis* RP62A.

Phage Andhra's capsid shape is icosahedral and the tail is tubular. Phage Andhra is estimated to have a capsid diameter of 42.7 ± 1.5 nm from Transmission Electron Microscopy (TEM) imaging (Figure 1A) (Cater et al., 2017). Another study reports that Andhra has a capsid of 50 nm in diameter and a tail of 40 nm in length (Hawkins et al., 2022).

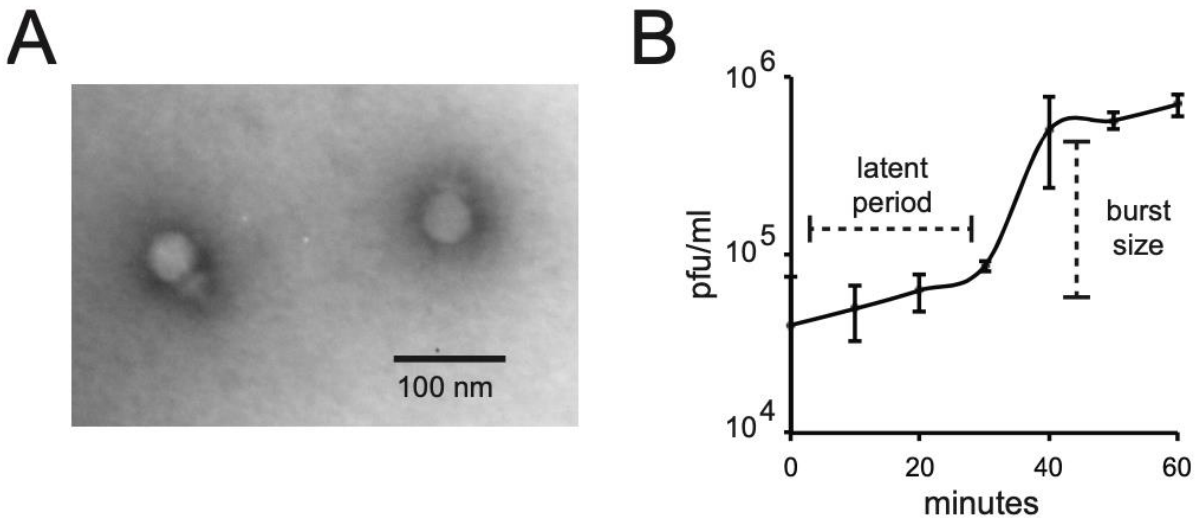

Figure 1. Phage Andhra: TEM Image and One-Step Growth Curve.

(A) This figure shows an image of Phage Andhra using Transmission Electron Microscopy (TEM) at X 200,000 magnification. Andhra was stained with uranyl acetate. (B) A one-step growth curve of Andhra growing with S. epidermidis RP62A is shown, with data being collected at 10-minute intervals (Cater et al., 2017).

The life cycle of phage begins when they lyse the bacterial cells. This life cycle can be shown in the form of a growth curve. A growth curve consists of the burst size and the latent period. Burst is defined when the phage releases its genome into the bacterial host cell. The burst size is the ratio of the final count of phage plaques to the initial count of phage plaques, which in most cases is also the greatest number of phage plaques divided by the lowest number of phage plaques counted over time. The latent period is defined as the time that occurs between phage adsorption and the beginning of the first burst (Cater et al., 2017). Figure 1B shows the one-step growth curve of Andhra, including the latent period, which takes about 30 minutes to occur, and burst size of 9.3 pfu/mL, which occurs right after the latent period, for phage Andhra (Cater et al., 2017). Phage Andhra is an example of an obligatorily lytic phage meaning that it undergoes vegetative phage replication that ends with lysis (Hobbs & Abedon, 2016).

Phage Therapeutics

Phage therapy is the use of phage as a potential remedy to treat bacterial infections in humans. The use of phage as a therapeutic method has been studied for many years and is becoming more apparent in the field as bacteria are starting to become more recalcitrant to antibiotics. Although new scientific technologies are emerging, efforts are still being made to modify antibiotics to prevent bacteria from developing complete resistance. Furthermore, phage are being studied to determine their therapeutic potential. There have been complications in the field where phage therapy is concerned. These complications arise from the phage not infecting the bacterial cells, causing no effect in the biomass of the biofilm. This could be a result of entrapped phage in the biofilm's pores or EPS matrix (Hansen et al., 2019).

Lytic phage are promising as a biofilm therapeutics due to their ability to lyse the bacterial host cells and replicate immediately after infection. The immediate replication of lytic phage and its narrow and specific host range is the reason for lytic phage emerging as the potential therapeutic to treat biofilms in the future (Hansen et al., 2019; Hatoum-Aslan, 2021).

Phage-Biofilm Interactions

The possible outcomes of phage treatment can lead to either an increase or decrease in height, porosity, and biomass of the biofilm. The effect that phage has on these biofilm properties is dependent on how the phage interacts with the components of the biofilm. Different outcomes occur depending on what biofilm constituents the phage interact with upon phage addition.

The effects of lytic phage on biofilm height, porosity, and biomass have been widely studied, with phage attacking bacterial cells through a different mechanism than antibiotics leading to a reduction or eradication of biofilm biomass (Fanaei Pirlar et al., 2022). Multiple studies have been done where the effects that phage have on the bacterial cells, pores, and EPS matrix of the biofilm are closely studied. Phage can infect the bacterial cells in the biofilm, which leads to a reduction

or eradication of biomass in biofilms. Lytic phage attack biofilms by contacting cell receptors on the bacterial envelope. The polysaccharides in the enzymes of the phage have depolymerization capability, which also allows the phage to reduce the biomass in phage-treated biofilms. The depolymerization capability can be directed towards the DNA or the polysaccharides in the EPS matrix of the biofilm, depending on the phage genome (Fanaei Pirlar et al., 2022). Phage can interact with the EPS matrix formed by bacteria in biofilms (Figure 2D). Phage can become entrapped in between the pore of the biofilms, where there are no bacterial cells or EPS matrix present (Figure 2C). Studies of these interactions are limited. Vidakovic et al. show that due to the phage interacting with EPS matrix components in *Escherichia coli* biofilms, there was not a significant change to biofilm biomass. However, when biofilms that did not produce these matrix components were grown with phage, there was an obvious decrease in biofilm biomass (Vidakovic et al., 2018). Some phage aggregate the matrix components of the biofilm to the point where nutrients that enhance biofilm growth, such as carbon and nitrogen, are released within the biofilm. The phage-induced aggregation in the biofilm may create favorable microenvironments where the bacterial cells and the EPS matrix in the biofilm continue to grow (Hansen et al., 2019).

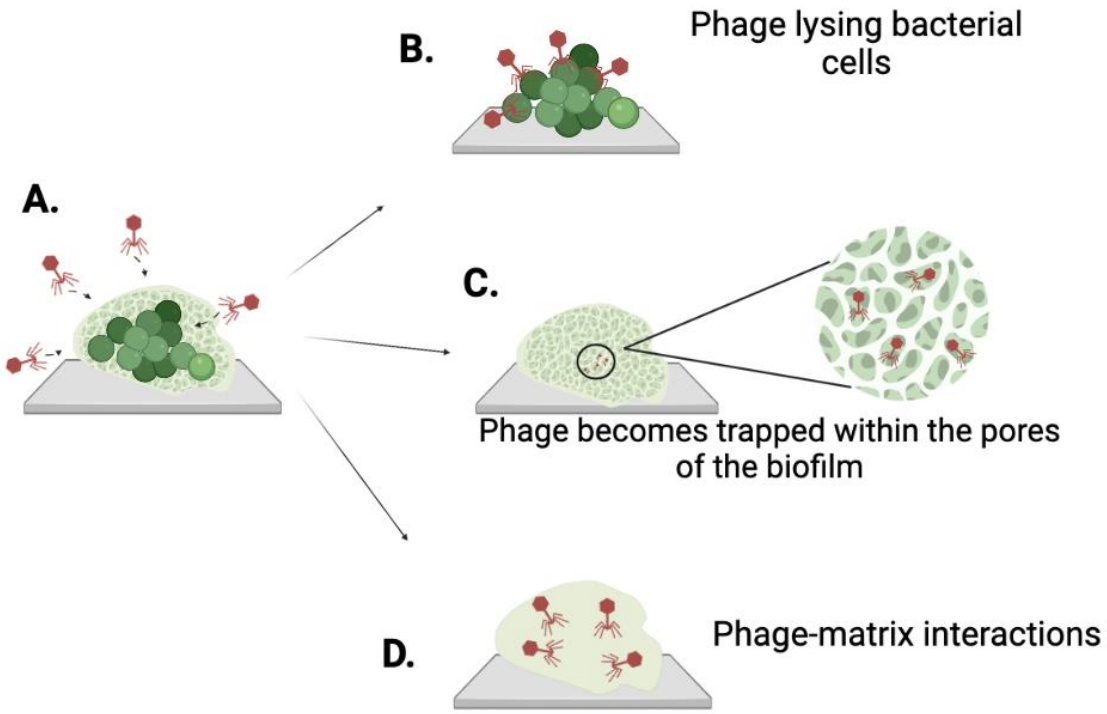

Figure 2. Phage-Biofilm Interactions.

Diagram of the different ways that phage can attack the different properties of a biofilm. (A) Representation of a biofilm on a surface and the phage being added to the biofilm. (B) When phage attack the biofilm, they can find bacterial cells to infect and propagate. (C) When phage penetrate

the biofilm, they can also find themselves within the porous areas of the biofilm, where there is no EPS matrix or bacterial cells to interact with. (D) When phage penetrate the biofilm, they can become entrapped within the components of the EPS matrix of the biofilm.

In studies where biofilms are treated with phage, the concentration of both phage and the bacterial cells in the biofilm must be known prior to phage treatment. In the field of phage therapy, multiplicity of infection (MOI) is used to define the ratio of the concentration of phage particles to the concentration of the bacterial cells in the biofilm. The use of MOI has been applied in other studies in the virology community. Although it is mentioned by several papers that MOI is an overly simplistic method to depict the ratios of concentration, it has been used by many studies to portray the ratio of infectious virions to cells in a culture (Shabram & Aguilar-Cordova, 2000).

The concentration and density of bacterial cells in biofilms prior to phage treatment is crucial to determine the effectiveness of phage therapy, but there is a lack of clarity in determining the MOI prior to phage treatment in the literature. One of the possible interactions between phage and *S. epidermidis* biofilms occurs when the phage viral particles infect and lyse the bacterial cells (Figure 2B). The phage particles attacking the bacterial cells can lead to reduction of biomass in the biofilm. This prediction can be made due to previous studies adding phage to established biofilms and measuring the effects on the biomass in the biofilm. Fanaei Pirlar et al. describe a reduction of biomass in a 24-hr established *S. epidermidis* biofilm right after 2 hours of phage treatment, with no biofilm regrowth in the remaining 22 hours. The reduction of biofilm was measured by determining the concentration of the bacteria in the biofilm in cfu/mL (colony forming units/mL). The MOI was not determined before phage treatment in this study (Fanaei Pirlar et al., 2022). Curtin and Donlan used catheters to replicate an *S. epidermidis* biofilm infection and treated the biofilm with phage for 24 hours. The MOI was not determined before phage treatment, however the concentration of the biofilm treated on the catheter was estimated using cfu counts and the concentration of the phage before treatment was estimated using plaque assays. By analyzing the cfu counts per area on the catheter before and during phage treatment, it was seen that the concentration of bacteria gradually decreased over 24 hours (Curtin & Donlan, 2006). In these studies, there is not a clear or definitive method for calculating the concentration or density of the bacteria before phage treatment. The lack of clarity on the concentration of the phage and the bacterial cells in the biofilm, before phage treatment, is important to address because this can have a great impact on the effectiveness of phage therapy. The lack of clarity in determining the MOI prior to phage addition makes it more difficult to replicate phage-biofilm experiments. If phage-biofilm experiments are difficult to replicate, then it will also prove difficult to compare the efficacy of the phage at different concentrations and compare the results between other studies and experiments in the literature. Additionally, there are no clear results on the effects that phage has on the different *S. epidermidis* biofilm properties such as the biofilm height, porosity, and biomass. Without a controlled method of defining the concentration of phage and

bacterial cells in the biofilm prior to phage addition, it is unclear how phage impacts the overall structure of the biofilm.

If phage have a greater burst size, they are capable of eradicating biofilm biomass. Complete eradication of biomass in the biofilm is seen when there are no bacterial cells present in the biofilm after phage treatment, leaving only the EPS matrix and media in the biofilm. Fanaei Pirlar et al. depict that with *S. epidermidis* 18, the high titer phage eliminated all presence of the bacterial cells in the biofilm after 10 hours. This was because of the high burst size of 3 pfu/cell with a latent period of 90 minutes with this strain of *S. epidermidis.* The bacterial cell concentration over time was portrayed in a time-killing assay. The MOI was not determined before phage treatment in this study (Fanaei Pirlar et al., 2022). In another study, Lungren et al. treated a static 24-hr *S. aureus* biofilm with phage and allowed both species to grow together for 24 hours. The MOI was not determined before phage treatment, however cfu and pfu counts were done to determine the seeding concentration of biofilm and the titer of phage before it was added to the biofilm. The results from this study showed a near complete eradication of the biofilm, only leaving 0.01% of biomass when compared to the control. This study conducted cfu counts to obtain the concentration after phage treatment. Although the biofilms in this study might not have been specifically *S. epidermidis*, this study allows some insight on one of the possible outcomes that may occur as a result of phage treatment to biofilms (Lungren et al., 2013).

Cfu counts can be a useful tool to calculate the bacterial cell concentration, yet there are some limitations that arise using this method. The number of colonies counted may not represent the actual number of bacterial cells in a sample as sometimes multiple bacterial cells clump together to form a single colony, leading to an overestimation of concentration. Some colonies can be bigger than others, which might cause the smaller colonies to not be counted, leading to an underestimation of concentration (Curtin & Donlan, 2006).

The effect that phage treatment has on biofilm biomass is complex and can vary depending on the MOI used and may be influenced by the components of the biofilm such as the EPS matrix and the pore structure. In the case that the phage particles become entrapped in the EPS matrix or the pores of the biofilm, the bacterial biofilm may continue to grow. The EPS matrix and the pores within the biofilm can serve as a defense mechanism that protects the bacterial cells against phage infection, which may result in the biofilm appearing to be undisturbed while it continues to grow. Lacqua et al. found that when *Escherichia coli* was grown with different strains of phage at MOIs varying from 0.1 to 100, some of the phage strains increased biofilm formation upon phage addition. In this paper, the biofilm sample was stained with crystal violet, which stains the EPS matrix of the biofilm. Using spectrophotometric determination, the absorbance of the biofilm sample was measured. A greater absorbance indicates a greater amount of biofilm in the sample (Lacqua et al., 2006). Henriksen et al. describes adding lytic phage to *Pseudomonas aeruginosa* flow-cell biofilms grown at 1, 24, and 72 hours. The MOI prior to phage addition was about 1000.

A confocal laser scanning microscope was used to obtain z-stacks of the biofilms at an objective of 63x/1.4. The image analysis software COMSTAT was used to observe that there was an increase of biomass in the biofilms (Henriksen et al., 2019). In both studies, the MOI prior to phage treatment was stated, however it was not clear how the MOI was determined. The concentrations for phage were stated as approximations and only the optical density at a wavelength of 600 nm (OD_{600}) was noted. Cfu counts were reported after phage treatment only. The ambiguity in the method to determine the MOI makes it difficult to analyze how the variation of MOI was conducted and controlled.

Through the analysis of multiple studies conducting phage treatments on biofilms, there are several limitations in studying the effect that phage has on the different properties of the biofilm. One of the limitations includes biofilm growth after phage addition. Without measuring the bacterial cell concentration before treatment and analyzing the biofilm structure after phage treatment, it is difficult to determine if there was any increase in biofilm growth caused by the phage treatment. By defining the biofilm height, porosity, biomass, and bacterial cell concentration before phage addition, the biofilm structure can be analyzed after phage treatment and can be compared to the values obtained prior to phage treatment to truly see how the phage impacted the biofilm structure. Another limitation in these studies includes the inaccurate calculation of MOI upon phage addition. MOI is the concentration of the phage over the concentration of the bacterial cells in the biofilm. Most studies include the concentration of phage but not the concentrations of the bacterial cells in the biofilm prior to phage addition. The inconsistent methods of calculating the MOI prior to phage addition allow for ambiguity in MOI calculations, making it unclear in the literature what this ratio truly signifies. By calculating the concentration of the phage and the bacterial cell concentration of the biofilm prior to phage treatment, ambiguity when determining the MOI can be diminished (Abedon et al., 2021).

Materials and Methodology

Bacteriophage and Bacteria Strains

Staphylococcal phage Andhra was used in this study. Phage Andhra is a lytic phage that was originally obtained from raw sewage (Cater et al., 2017). Andhra is in the bacteriophage family *Podoviridae.* Phage Andhra is one of 10 reported bacteriophage where *S. epidermidis* is the bacterial host, however Andhra is the first phage coming from the family *Podoviridae* (Cater et al., 2017).

The bacteria strain used in this study is *S. epidermidis* RP62A (American Type Culture Collection (ATCC) 35984). This strain of bacteria originated from an outbreak of intravascular catheter-associated sepsis biofilm infections in 1979 to 1980 (Gill et al., 2005). *S. epidermidis* RP62A was chosen for this study as it is a bacterial host for lytic phage Andhra (Cater et al., 2017).

Bacteria and Biofilm Growth Conditions

Planktonic *S. epidermidis* was grown overnight in a liquid culture prepared in tryptic soy broth (TSB) supplemented with 1% weight glucose, which will be referred to as TSB_G. The overnight liquid culture was grown on a shaker table at a speed of 180 rpm and incubated at 37^{o}C for 12 hours. When phage were cultured with planktonic *S. epidermidis* RP62A, 5 mM of Calcium Chloride ($CaCl_2$) was added to TSB and was used as growth media. The TSB media supplemented with $CaCl_2$ will be referred to as TSB+$CaCl_2$. The addition of $CaCl_2$ to the growth media enables the phage to be more susceptible to interacting with the bacterial cells. Due to $CaCl_2$ being a divalent metal ion, the virion receptors on the phage are weakened allowing for an increased phage adsorption rate. The positively charged $CaCl_2$ ion interacts with the negative charge of the phage making the phage a neutrally charged particle entering the biofilm (Chaudhry et al., 2014; Olson & Horswill, 2014).

S. epidermidis biofilms were grown for 24-hours prior to the addition of phage. Biofilms were grown by culturing bacteria in TSB_G statically at 37^{o}C for 24 hours. The initial seeding concentration of bacteria was 5 x 10^5 cells/mL based on the MacFarland standard with an OD_{600} (optical density at a wavelength of 600nm) value of 0.1. Biofilms were grown in 8 well Nunc™ Lab-Tek™ II Chambered Coverglass (ThermoFisher Scientific) with a seeding volume of 400μL. Phage were added to biofilms grown for 24 hours to study the effect of MOI on biofilm development.

Phage Growth and Propagation Conditions

Low titer, or low concentration, phage lysate solutions were produced for obtaining phage plaques prior to the creation of a high titer, or high concentration, phage lysate. To create a low titer phage lysate, a small scraping of a frozen stock of phage was swirled in a 1:100 dilution of overnight *S. epidermidis* RP62A liquid culture and incubated overnight (6-12 hours) on a shaker table at a speed

of 180 rpm and a temperature of 37ºC. The overnight liquid culture was prepared the night before by obtaining a colony from a bacterial plate and swirling it in 10-20 mL of TSB+$CaCl_2$. This solution was then centrifuged for 2 minutes at 12,000 rpm and filtered through a 0.45 μm syringe filter. Heart Infusion Agar (HIA) is prepared at half the concentration that is presented on the manufacturer's label. This solution of HIA is referred to as the 0.5x concentration HIA top agar. To produce a plate with individual plaques of phage, 4 mL of top agar, 100 μL of overnight host liquid culture, and 30 μL low titer phage lysate are mixed together. The agar mixture is then poured on a TSA+$CaCl_2$ plate. This plate is then placed in an incubator at 37ºC and allowed to grow overnight (12 hours). This plate will produce individual plaques of phage that can be seen on top of a lawn of bacteria.

High titer phage lysate is needed to enable controlled addition of high concentrations of phage to biofilms. High titer phage lysate is also used to study the phage size and zeta potential. To create a high titer phage lysate, a plate must first be grown with low titer phage lysate to obtain a plaque from a plate. A plaque is added to 2 mL of TSB+$CaCl_2$, vortexed for 10 seconds and centrifuged for 2 minutes at 12,000 rpm. To increase the concentration of the phage, a diluted solution of the HIA top agar must be prepared. The diluted solution of HIA top agar will be referred to as sloppy agar. To create a solution of sloppy agar, 1.3g of HIA must be poured into 100 mL of DI water. The supernatant of the centrifuged phage mixture is then mixed in a solution of 7 mL of sloppy agar and 100 μL of overnight liquid culture. This mixture is then poured on a TSA+$CaCl_2$ plate and grown for 24 hours at 37ºC (Figure 3). Once the phage has grown on the plate, the layer of sloppy agar containing the phage is then scraped off into 25 mL of TSB+$CaCl_2$, so that it can be vortexed and centrifuged for 5 minutes at 10,000 x g. The supernatant of this mixture is then filtered through a 0.45 μm syringe filter. This produces the high titer phage lysate for phage treatment to the biofilm.

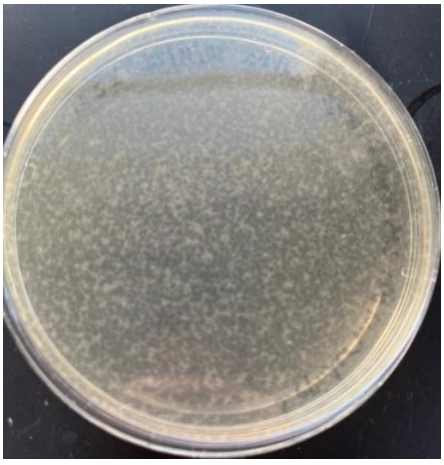

Figure 3. TSA+$CaCl_2$ plate with sloppy agar.

The clear spaces in the plate signify that there is a high concentration of phage on the plate. The white spaces represent the portion of the lawn of bacteria that the phage did not infect.

The concentration of the high titer phage lysate was determined by plating serial dilutions of the high titer phage lysate on TSA+$CaCl_2$ plates. To perform these serial dilutions the plate first needs to be split into 8 different sections, first section marked "x" to maintain as a control section and the rest numbered from 2-8 (Figure 4). The numbers on the plate represent the degree of dilution of the original phage solution. Eight microcentrifuge tubes were labelled 1-8 and set up on a tube rack with 90 μL of TSB+$CaCl_2$ in each tube. In the first microcentrifuge tube, 10 μL of the high titer phage lysate was added. To mix the media with the high titer phage lysate well, it was pipetted up and down a couple times. Next, 10 μL of the solution in the first microcentrifuge tube was then pipetted into the second microcentrifuge tube and pipetted up and down to mix well. This was repeated until there was 100 μL of media in the last (8) microcentrifuge tube. These dilutions created a 10^2 dilution of high titer phage lysate in TSB+$CaCl_2$ in the second microcentrifuge tube, a 10^3 dilution of high titer phage lysate in TSB+$CaCl_2$ in the third microcentrifuge tube, and so on.

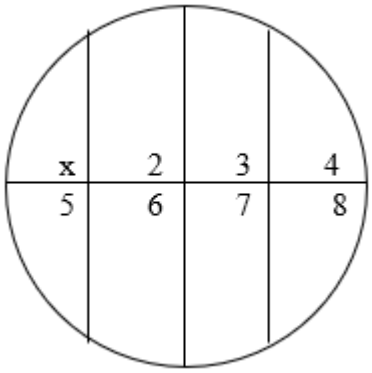

Figure 4. The eight different sections marked and labelled on a plate.

Before the different serial dilutions of the phage were pipetted onto the plate, 4mL of top agar and 100 μL of overnight liquid culture are mixed together and poured onto the plate. The top agar must be left to harden for about 10 minutes before the serial dilutions are pipetted onto the plate.

It is important to note that the overnight liquid culture for the bacterial lawn must have and OD_{600} greater than 1.2. If the optical density is lower than this value, the bacteria will not form a lawn on the plate and then the phage will not have enough host cells to infect, causing no formation of phage plaques. It is also crucial to let the agar harden for at least 10 minutes before proceeding to pipette the dilutions on the plate. If the dilutions are pipetted on the plate before 10 minutes, the top agar will be closer to a liquid consistency causing the pipetted phage to disperse throughout the plate. This will appear as bacterial colonies scattered over a plate of agar and not showing any evidence of the phage that was pipetted in the different sections (Figure 5).

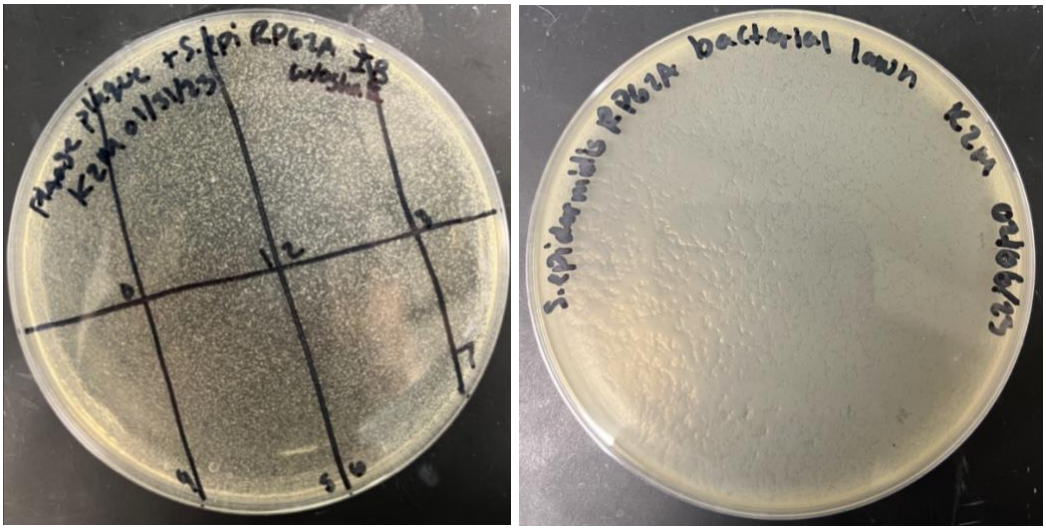

Figure 5. Failed Concentration Plate and Bacterial Lawn.

(Left) A concentration plate where the bacterial liquid host culture was grown for 6 hours and the top agar was not left to harden for a full 10 minutes, so the concentration of the bacteria was not high enough and the phage did not stay in the pipetted circles due to the unhardened top agar. (Right) A representation of what the bacterial lawn is meant to look like without plating any phage.

After the serial dilutions of the phage were performed, 5 μL of each dilution was pipetted onto the respective section on each plate, with nothing being pipetted on the section marked as "x" to represent the control. The plate was incubated at 37°C for 24 hours to allow the phage to propagate in the bacterial lawn. The dilution with countable plaques after 24 hours was identified and plaques were counted. The concentration of phage within the high titer phage lysate in pfu/mL was then calculated using:

Equation 1: Phage Concentration

$$(\#\ of\ plaques) * 10^{d} * 200 = pfu/mL \quad (1)$$

In equation 1, the "# of plaques" represents the number of countable plaques or clear circles in the section of the plate being counted. The letter "d" represents the dilution factor for the section of the plate that is being used to count the plaques. "d" is determined by the specific dilution of the chosen section of the plate. The number 200 takes in account the volume of the high titer phage lysate (5 μL) and the unit conversion to mL. An example of what the plate and plaques look like when calculating the concentration can be seen in Figure 6. In Figure 6, there are no phage in the control quadrant "x". In quadrants 2-4, the concentration of phage is too high to be able to count individual plaques. In quadrant 5, there are countable plaques. In quadrants 6-8, there are too few phage to determine a concentration.

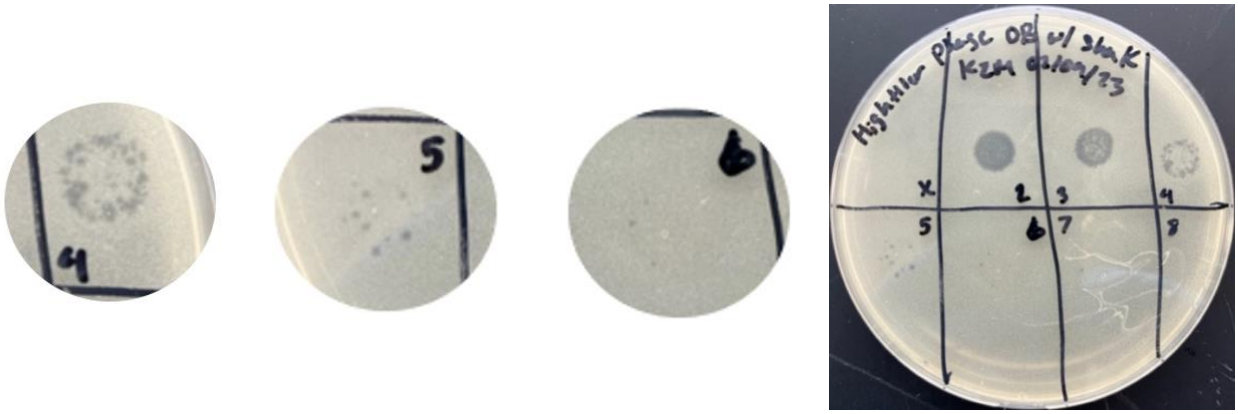

Figure 6. Example of a 24-hour plate for calculating phage concentration.

Quadrant 5 has countable plaques therefore it is a good representative quadrant to choose and determine phage concentration. There are too many plaques in quadrant 4 to clearly count the number of plaques and not enough plaques to represent an accurate concentration in quadrant 6.

This method of calculating the phage concentration provides an estimate of phage concentration; however, the method may provide an over or underestimation of phage concentration. There may be some phage particles that have not completed lysis, therefore not displaying the true amount of phage in solution, which leads to an underestimation of the true phage concentration in the phage lysate. When the phage infect the bacterial cells on the bacterial lawn, they may aggregate or clump together, appearing as one big plaque instead of the different number of plaques it is truly representing. The aggregation of the phage particles may lead to an overestimation of the phage concentration (Marianne Poxleitner, 2018).

Characterization of Size and Charge of Phage

To find the particle size and charge of the phage, the sloppy agar was scraped off into 25 mL of TSB_G and was vortexed for 5 minutes and centrifuged at 10,000 x g for 5 minutes, The supernatant was filtered through a 0.45 μm syringe filter, producing a high titer phage lysate. The high titer phage lysate in TSB_G was prepared for phage size and zeta potential measurements using a Malvern Zetasizer (Southborough, MA).

To determine the particle size of the phage, the zetasizer uses dynamic light scattering (DLS) to detect the particles in a sample and determine the size. DLS uses lasers to detect the particles in the sample and takes in account the Brownian motion of the particles to calculate the average size of the particles in the solution. Brownian motion describes the movement and collisions of particles in solution. The zetasizer considers the Brownian motion and the light being reflected off the particles to produce a correlation of the intensity reflected from the particles over time. With the

movement of the particles and the DLS method that the zetasizer utilizes, the average particle size of the phage is calculated (Malvern, 2013).

The phage in TSB_G was used to measure the size and zeta potential. Generally, samples that are inputted into the zetasizer for particle size measurements use water as the dispersant. However, when the high titer phage lysate was suspended in TSB+$CaCl_2$ and water, the zetasizer displayed errors such as "Refer to quality report". This was due to the presence of sedimenting particles, high polydispersity, and presence of large particles/aggregates/dust. The phage particles could also be aggregating with each other or the other larger particles that are present in the sample, which can be another reason for an error message to be displayed. The polydispersity index (PDI) of a sample is defined as how broad the distribution of the average particle size calculated is. The more variation that is computed as the average particle size, the greater the distribution of the particle size. A greater distribution is represented by a greater width and a greater PDI value. The PDI value must be below 0.5 for the data computed by the zetasizer to accurately calculate and define the average particle size. An example of good quality and bad quality results can be seen in Figure 7.

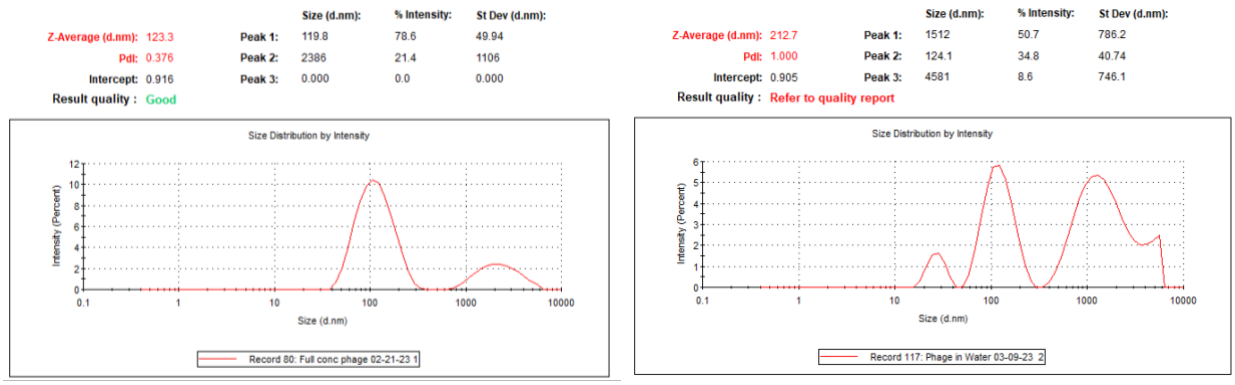

Figure 7. Comparison of Zetasizer Results.

(Left) An example of a good quality result of one run calculating the average particle size of phage in TSB_G computed by the zetasizer. The good quality result is reflected by the low PDI. (Right) An example of a bad quality result of one run calculating the average particle size of phage in water computed by the zetasizer. The bad quality result is reflected by the high PDI possible due to larger particles in the sample and aggregation between the phage particles.

The minimum concentration required for a zetasizer measurement is based on estimating the particle density in the sample and knowing the range of the particle diameter in the solution being examined by the zetasizer. The plot in Figure 8 was used to ensure that the high titer phage lysate in TSB_G was concentrated enough for zetasizer measurements. In one previous study, utilizing TEM, the capsid size of phage Andhra was found to be 42.7 ± 1.5 nm in diameter (Cater et al., 2017). In another study, an EM with a Gatan K3 detector was used to find that the capsid size of

phage Andhra was 50 nm in diameter and the tail of phage Andhra was 40 nm long (Hawkins et al., 2022). Therefore, assuming that the particle size of phage Andhra is around 100 nm and that the high titer phage lysate contains a high density of phage particles, over 1 g/l (gram/Liter), we can determine that the minimum concentration of phage that should be used to calculate particle size and charge in the zetasizer is around $1 * 10^7$ particles. The concentration of the high titer phage lysate in TSB_G was $7.4 * 10^8 \pm 1.1 * 10^9\ pfu/mL$, thus the high titer phage lysate was concentrated enough to find the particle size and zeta potential of phage Andhra.

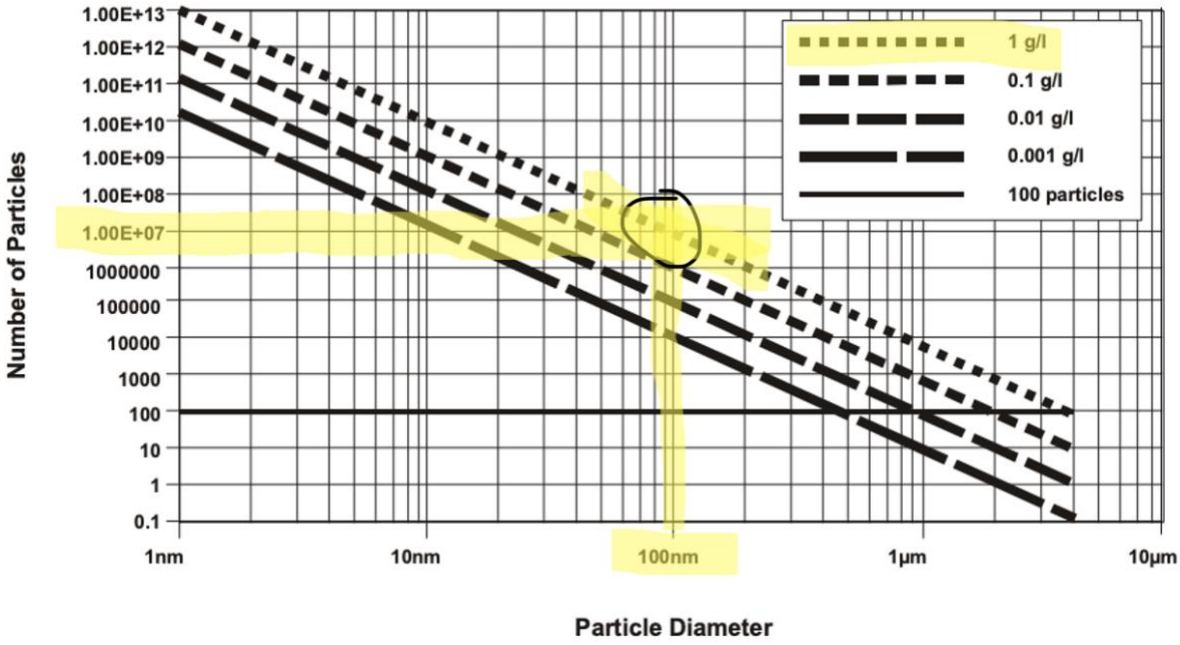

Figure 8. Minimum Concentration Plot for the Zetasizer.

Plot used to determine the minimum concentration that a sample must be before placing it in the zetasizer (Malvern, 2013).

The dispersant used to evaluate the particle size and zeta potential of phage Andhra was TSB_G. Therefore, the appropriate solvent parameters must be used to account for the components in TSB_G (Table 1). Setting these parameters accurately are essential to calculate the size and zeta potential of phage Andhra. By inputting the concentration of each component, the zetasizer will calculate the viscosity and refractive index. The viscosity is significant as this value affects the accuracy of particle size and zeta potential measurements. The presence of the other components, such as the sodium chloride and glucose contribute to the bulk viscosity. By considering the contribution of these components through the viscosity value of the dispersant, the particle size and zeta potential of phage Andhra were obtained.

Table 1. Parameters used in the zetasizer for TSB_G			
Component	**Concentration (M)**	**Viscosity (cP)**	**Refractive Index**
Water	--	0.88718	1.33000
Sodium Chloride	0.08	0.00857	0.00082
Glucose	0.24	0.12529	0.00612

The zeta potential of the phage was calculated to obtain the charge of the phage. The zeta potential is calculated by measuring the velocity of the phage using Laser Doppler Velocimetry (LDV) to find the electrophoretic mobility, or velocity of the particles in solution. LDV uses light beams that omit light throughout the sample, capturing the reflections of the phage. By keeping track of how many times the zetasizer detects a reflection and the frequency of these detections, the velocity of particles moving through the sample is calculated using LDV. The charged zetasizer cuvette (Figure 9) allows for the particles to gravitate towards one of the ends of the cuvette. At one end of the cuvette there is a positively charged electrode and at the other end there is a negatively charged electrode. A positively charged particle will gravitate towards the negative electrode, while a negatively charged particle will gravitate towards the positive electrode. The light beams omit a scattering intensity signal as the particles move within the capillary, which is used to compute the electrophoretic mobility. The viscosity and dielectric constant are automatically calculated by the zetasizer once the concentration of each component of the dispersant are added to the list of parameters. Henry's function is determined either by the Smoluchowski approximation or the Huckel approximation. The Smoluchowski approximation states that Henry's function is 1.5 when working with particles that are larger than 0.2 μm dispersed in electrolytes containing more than 10^{-3} M salt. The Huckel approximation states that Henry's function is 1.0 when working with smaller particles in low dielectric constant media. Since phage particles are generally under 0.2 μm, or 200 nm, Henry's function would be 1.0. The velocity calculated using the LDV technique is the electrophoretic mobility. The electrophoretic mobility is then applied to Henry's equation:

Equation 2: Zetasizer – Electrophoretic Mobility

$$U_E = \frac{2\varepsilon z f(\kappa a)}{3\eta} \tag{2}$$

where the electrophoretic mobility (U_E) is used along with the dielectric constant (ε) of the media, Henry's function ($f(\kappa a)$), and the viscosity (η) to compute the zeta potential (z).

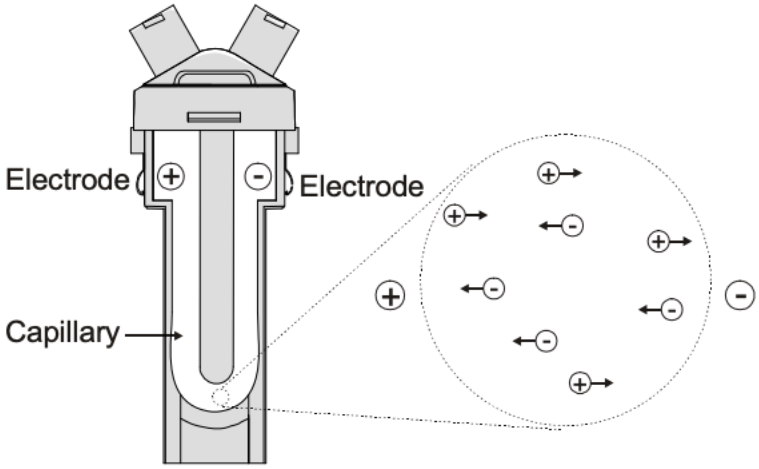

Figure 9. Zeta Potential Cuvette.

The charged cuvette used to determine the zeta potential of phage in solution using the zetasizer (Malvern, 2013).

Quantification of MOI of phage to bacteria within biofilms

The MOI is the ratio of viral particles to infection targets, where the viral particles are synonymous to the phage and the infection targets are synonymous to the bacterial cells in the biofilm. The MOI ratio that is typically used represents the value where all viral particles can infect all the cells in a culture (Shabram & Aguilar-Cordova, 2000). In this paper, I define MOI as the ratio of the concentration of phage particles to the concentration of bacterial cells in the biofilm. However, some bacterial cells in the biofilm may not be susceptible to phage infection. To calculate the MOI before phage treatment, the concentration of the phage and the bacteria within the biofilm must be known prior to phage treatment. The concentration of the high titer phage lysate was found using a serial dilution method, which is a well-established method. The concentration of bacteria in the 24-hour biofilm was estimated by quantifying the local number density of bacteria in the biofilm and the total biofilm biomass and estimating the total number of bacterial cells in the biofilm. The local number density of bacteria and the total biofilm biomass were determined using confocal laser scanning microscopy (CLSM) coupled with image analysis (see CLSM Imaging and Analysis of Biofilms section below for additional details). After obtaining estimates of the concentrations of phage and bacteria the MOI was calculated using Equation 3:

Equation 3: Multiplicity of Infection (MOI)

$$MOI = \frac{\left(\frac{pfu}{mL}\right) * (volume)}{total\ \#\ of\ cells} \quad (3)$$

where pfu/mL represents the concentration of the high titer phage lysate, the volume in the numerator represents the volume of the high titer phage lysate added to the biofilm, and the total number of cells represents the total number of bacterial cells in the biofilm.

The bacterial cell concentration is significant to my work as it is needed to calculate the MOI prior to phage treatment. Calculating the bacterial cell concentration must be done in three different steps. First, the local number density of the bacterial cells in the biofilm must be known. Secondly, the volume that the biofilm is taking up must be known. Lastly, with the calculated values of the biofilm volume and the local number density, these can be multiplied together to obtain the total number of bacterial cells in the biofilm.

Phage Treatment of Biofilms

Phage Andhra were added to a *S. epidermidis* RP62A biofilm that was grown for 24 hours. Phage were then cultured with *S. epidermidis* biofilms for 24 additional hours. After the biofilm was grown for 24 hours, the remaining media was extracted carefully with a pipette and replaced with an aliquot of 400 μL of high titer phage lysate in TSB+$CaCl_2$. The different concentrations of phage added to the biofilm were chosen to be $4.3x10^7$ pfu/mL to give an MOI of 0.07, $4.3x10^8$ pfu/mL to give an MOI of 0.67, and $7.4x10^8$ pfu/mL to give an MOI of 1.16 (Table 2). The MOI is the ratio between the concentration of phage and the concentration of the bacteria in the biofilm. The phage and biofilm were grown statically in a 37°C incubator for an additional 24 hours, 48 hours total. The changes to the height, porosity, and biomass of the biofilm were then evaluated for each MOI. Control biofilms with no phage were grown for 48 hours with a media exchange at 24 hours, where 400 μL of TSB+$CaCl_2$ was added.

Table 2. Specified Phage Concentrations Added to Biofilm for Different MOIs

Biofilm Experiments	Phage Concentrations (pfu/mL)
MOI = 0.07	$4.3x10^7$
MOI = 0.67	$4.3x10^8$
MOI = 1.16	$7.4x10^8$

CLSM Imaging and Analysis of Biofilms

To observe biofilms using the CLSM, the biofilms must first be stained with 1 μM of Syto9 fluorescence dye. This process should be carried out 30 minutes prior to imaging, and the biofilms should be wrapped in tin foil or placed in a dark room to avoid photo-bleaching of the sample. The Syto9 dye is used to stain the living cells within the biofilm and is excited at a wavelength of 485 with an emission at 495. The two different objectives used with the CLSM are 10x with a numerical aperture (NA) of 0.4 and 63x with oil immersion with a NA of 1.4. The area of the images are 512 x 512 pixels. At 10x, the step size was 1 μm and the pixel size was 3.03 μm/pixel. At 63x the step size was 0.08 μm, with a pixel size of 0.08 μm/pixel, and a zoom factor of 6.02. The CLSM obtains

these images using a laser light under the slide, shown in the highlighted area in Figure 10, to scan and capture images of the sample. Each biofilm was imaged at the 10x and 63x objectives. At each objective, five different z-stack images were taken. The areas chosen to image for each biofilm were in the four corners and the middle of the biofilm grown in the well, as seen in the bottom view of the well in Figure 10. I chose to obtain image volumes at these different locations in the biofilm well to enable consistent data collection across biofilm experiments. A total of 3 replicates of each experimental condition was done. This brings the total to 15 z-stack images being analyzed per experimental condition. A summary of the imaging process can be seen in Figure 10.

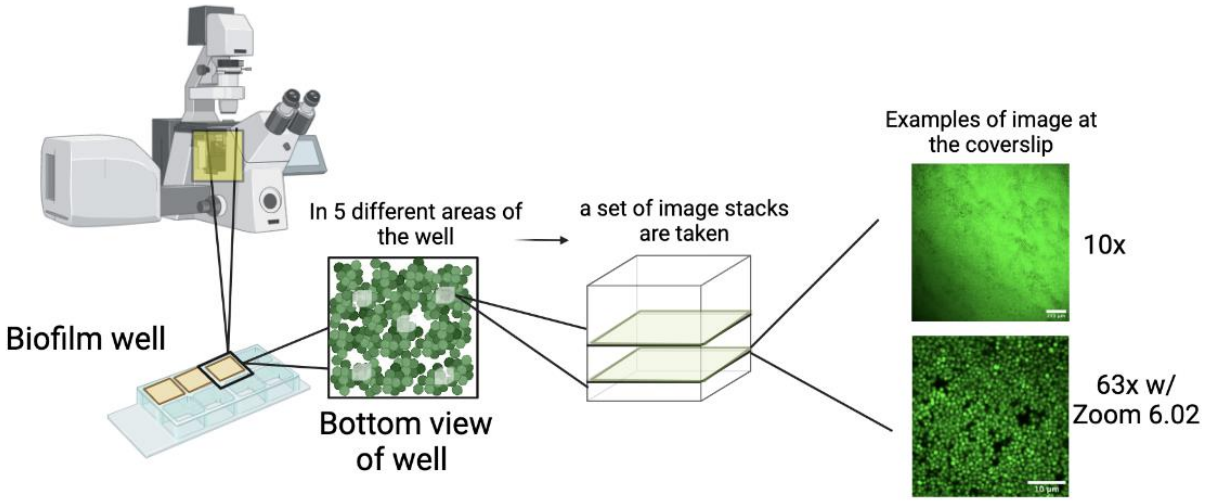

Figure 10. Schematic of the workflow for imaging biofilms using the CLSM.

Estimation of Bacterial Cell Concentration Within a 24-hour Biofilm

To estimate the number of cells in a 24-hour biofilm, the local number density of the biofilm and the total biofilm volume was computed. On the CLSM, z-stack images were taken using a 63x objective with oil immersion and a zoom magnification of 6.02. The step size used was 0.08 μm generating about 240 different z stack images. The pixel size was 0.08 μm/pixel. The dimensions of these images were 80 x 80 μm. After the pictures were taken, the image analysis software, Trackpy, was used to find the local cell density within the biofilm. The computer programming language Python was used in conjunction with Trackpy (Dan Allan, 2021; Kao et al., 2021), a particle tracking toolkit, to identify the location of the bacteria throughout the biofilm. The Crocker-Grier algorithm was used to identify the bacterial cells in the biofilm throughout the image stack (Crocker & Grier, 1996). The diameter of the bacterial cells must be defined, for the code to accurately identify the bacterial cells within a set area in the image volume of the biofilm. The diameter and separation must be inputted into the code in pixel units. The value that was inputted for the diameter of the bacterial cells was 9 pixels, which is equivalent to 720 nm. The separation input defines the minimum separation between the center of each bacterial cell that Trackpy

identifies. The value for the separation was 7 pixels, which is equivalent to 560 nm. Trackpy uses these parameters to calculate the number of bacterial cells in the image volume.

Once the number of bacterial cells within the image volume is determined, the number of bacterial cells is divided by the size of the image volume. This gives the local number density of the bacteria in the biofilm (Equation 4).

Equation 4: Local Density of Biofilm

$$Local\ \#\ density\ of\ biofilm\ (\rho) = \frac{\#\ of\ bacterial\ cells}{size\ of\ image\ volume} \quad (4)$$

To calculate the total number of bacterial cells in the biofilm (Equation 5), the local number density is multiplied by the total biofilm volume, which is computed in Equation 7. A visual representation of the image volume used to calculate the local number density of the biofilm is seen in Figure 11.

Equation 5: Total Number of Bacterial Cells in Biofilm

$$Total\ \#\ of\ cells\ in\ biofilm = Total\ biofilm\ volume * \rho \quad (5)$$

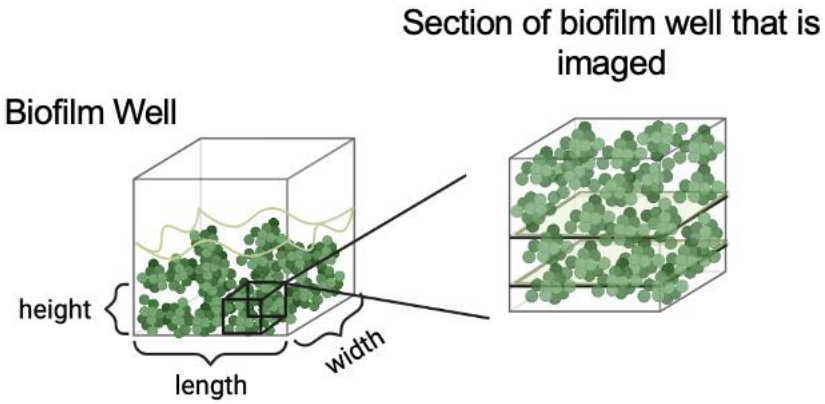

Figure 11. Schematic visualization of regions of the biofilm that are imaged to calculate the local number density.

Estimation of the Pore Size of Biofilms

The pore size of biofilms is an important characteristic that can affect the efficacy of phage therapy. However, there are limited studies that have quantified the pore size of *S. epidermidis* biofilms. Utilizing the image processing software ImageJ, I estimated the average size of the pores in 24-hour biofilms. The image volumes obtained at the objective 63x with a zoom magnification of 6.02 were used for this analysis. Only the first 10 μm of the biofilm were used for this estimation since the quality of the image volume starts to decrease closer to the media interface. The image volume

is thresholded to a value of 34, which was the average threshold best suited for all 15 image volumes at this objective. Thresholding the image volumes produces a binary image volume, meaning that the image volume only becomes black and white, where white represents the biofilm and black represents the proportion of the biofilm that is porous. Once the threshold is set, the "Analyze Particles" function in ImageJ was used to display the count, total area, average size, major axis, and minor axis of the pores in the biofilm. The count represents the number of pores calculated per image volume. The total area represents the total area of the biofilm that is porous. The average size is the average size of each pore that the software calculates. The major axis represents the longest diameter of the pore, and the minor axis represents the shortest diameter of the pore. The average of these values using the 15 different image volumes was used for this analysis. Finding the size of the pores allows for a better comparison and a better understanding of the interactions of the phage particles and the 24-hour biofilms.

Image Analysis of Gross Structure of Biofilms

Computing the height, porosity, and biomass of biofilms is important to my analysis because I can determine the ability of phage Andhra to reduce the thickness of the biofilm, penetrate the biofilm, and eradicate the bacterial cells in the biofilm. Using COMSTAT, I calculate how these properties change when different MOIs are treated to the biofilms. To assess biofilm gross structure, height, porosity, and biomass were determined using COMSTAT, which is an image analysis software that uses the computer programming language MATLAB to quantitatively analyze biofilm image volumes obtained from CLSM. COMSTAT uses connected volume filtering (CVF) to remove any elements in the image volume that are not considered biomaterial and to filter out background noise (Figure 12) (*COMSTAT*; Heydorn et al., 2000; Vorregaard, 2008). On the CLSM, z-stack images were taken using the 10x objective, a step size of 1 μm, and a total of 30 steps for a total height of 30 μm. The images contain 512 x 512 pixels with pixel sizes of 3.03 μm/pixel and total dimensions of 1553.03 μm x 1553.03 μm x 30 μm.

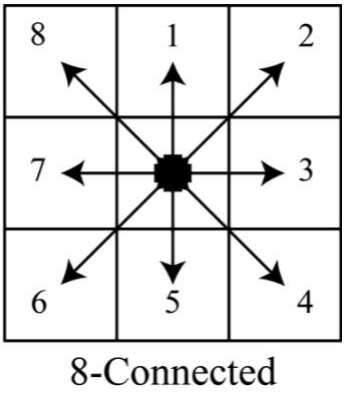

Figure 12. Visual representation of 8-connected expansion.

This diagram shows the 8-connected expansion method used in CVF. After applying a threshold, if COMSTAT detects biomaterial in any of the 8 pixels surrounding the main pixel it will detect that as biofilm.

Before analyzing the images on COMSTAT, a threshold must be determined for the image volumes. Thresholding transforms the image slices in the z-stack to binary images, where white represents the biofilm and black represents no biomass (Figure 13). When COMSTAT analyzes the binary image, it defines the white pixels as biomaterial. Once one white pixel is detected, the CVF method (Figure 14) allows COMSTAT to look at all the surrounding pixels. If any of the surrounding pixels are white, or contain biomaterial, it will detect it as biofilm. This process continues until a white pixel is reached that detects no surrounding pixels to contain biofilm.

A threshold analysis was done on 15 different image z-stacks to determine an average threshold value for the image volumes at 10x. The average threshold value best suited for all the different z-stack images at this objective was chosen to be 40. Before running the code, the pixel count, Z-step size, image dimensions, number of images in image volume, and threshold value must be defined (Table 3). COMSTAT can compute average biofilm height, the biomass, the height distribution, and the porosity vector. The height distribution calculates the number of pixels where biomass is detected at each image slice in the image volume. The porosity vector is the percent porosity that the code computes at each image slice in the stack. COMSTAT defines porosity as void space, or pixels that do not contain any biomaterial. The biomass is a calculation of the volume of the biofilm per unit area, as seen in Equation 6:

Equation 6: COMSTAT – Biomass

$$Biomass = \frac{V}{a} = \frac{[\mu m^3]}{[\mu m^2]} \quad (6)$$

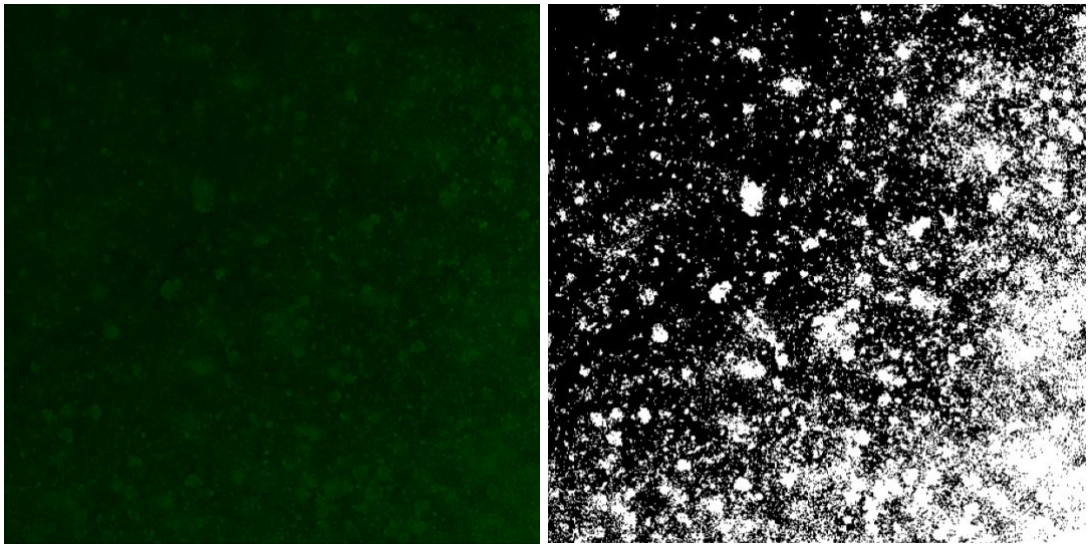

Figure 13. Thresholded Images at 10x objective.

(Left) An image from a 24-hr biofilm stained with Syto9 (green) at 20 μm, obtained at 10x. (Right) The thresholded version of the image on the left, where white represents the biofilm biomass and black represents no biomass.

Table 3. Parameters used in COMSTAT

	Pixel Count	Z-step size	Image Dimensions	Image #	Threshold Value
10x	512	1	1553.03	30	40

Due to a wide range in thresholding, the average biofilm height value computed by COMSTAT consistently underestimated the height of the biofilm. This was confirmed by qualitatively estimating the height of the biofilm visually. Therefore, I chose a method to identify the maximum height of the biofilms more accurately. By looking at the height distributions of the biofilms, the maximum height calculated by COMSTAT is greater than the actual biofilm height for all experimental replicates. COMSTAT is overestimating the height because it is assuming that the biofilm is evenly distributed across the substrate, like a perfect cube, however this is not the case. Biofilm growth is not uniform, therefore the maximum height computed by COMSTAT is an overestimate of the biofilm height. To address this issue in my image analysis, I have removed 1.3% of the image biomass from the calculation of the biofilm height as lowest average error in height was when 1.3% of pixels were omitted from the maximum height (Table 4). To determine the lowest error, omission of 0.01% to 1.6% of the tallest pixels from height determinations were considered (Table 5). Of note is that the 24-hour biofilm experiments and the experiments done at MOI=1.16 that had lower errors were done closer to the end of the study. My skill and consistency in imaging may have improved over the course of the study.

Table 4. Error Analysis For Choosing an Average Maximum Height of Biofilms

Biofilms	100% (Max height)	99.99%	99.9%	99%	98.7%	98.4%
MOI=0 24 hr	0.0484	0.0230	0.0622	0.1774	0.1843	0.1982
MOI=0 (Control) 48 hr	0.1741	0.1583	0.1319	0.0317	0.0132	0.0559
MOI=0.10 48 hr	0.1433	0.1322	0.0909	0.0275	0.0110	0.0028
MOI=1.0 48 hr	0.2460	0.1877	0.1165	0.0485	0.0356	0.0324
MOI=1.16 48 hr	0.0490	0.0074	0.0074	0.0956	0.1029	0.1152

Average Error	0.1322	0.1017	0.0818	0.0762	**0.0694**	0.0808

Table 5. Average Maximum Height of Biofilms in μm

Biofilms	**Visual Estimate**	**0% (Max height)**	**0.01%**	**0.1%**	**1%**	**1.3%**	**1.6%**
MOI=0 24 hr	28.9	30.3	29.6	27.1	23.8	23.6	23.2
MOI=0 (Control) 48 hr	25.3	29.7	29.3	28.6	26.1	25.6	23.9
MOI=0.07 48hr	24.2	27.7	27.4	26.4	24.9	24.5	24.1
MOI=0.67 48 hr	20.6	25.7	24.5	23.0	21.6	21.3	21.3
MOI=1.16 48 hr	27.2	28.5	27.4	27.0	24.6	24.4	24.1

With the percent justification of choosing the maximum height, the porosity value, or the proportion of the biofilm that does not contain biomaterial, for each biofilm experiment was calculated by taking the average porosity at the specified maximum height of each biofilm. Once the height and average porosity values are calculated, the total biofilm volume can be calculated using equation 7:

Equation 7: Total Biofilm Volume

$$Total\ biofilm\ Volume = height * length * width * (1 - porosity) \quad (7)$$

In equation 7, the height is given by COMSTAT, the length and width represent the dimensions of the well area that the biofilm was grown in, which is 0.7 cm^2 or $7x10^7$ μm^2, and the porosity value is calculated as the average porosity in the biofilm with the values given by COMSTAT.

This protocol was followed for analysis of phage-treated biofilms, as well.

Statistical Analysis

Biofilm height, porosity, and biomass results were analyzed with one-way ANOVA (Analysis of variance) when determining the effects that phage has on the biofilm structure. Tukey's HSD (historically significant difference) is a post-hoc test that was conducted to determine which experiments had significantly different means. The sample size for all the biofilm experiments was 15 image volumes obtained from 3 different experimental replicates. For the height, porosity, and

biomass data, the one-way ANOVA statistical test was run with multiple comparisons, where the mean of each experiment was compared with the mean of every other experiment.

Results and Discussion

Characterizing phage and determining a controlled method of calculating MOI prior to phage treatment is crucial in evaluating their potential as a therapeutic agent for biofilm infections. The significance of characterizing the phage is to study how the size and zeta potential will affect penetration into the biofilm and evaluate the potential of phage as a therapeutic agent for biofilm infections. Defining a controlled method to calculating the MOI prior to phage treatment gives insight as to how different concentrations of phage impact the different properties of the biofilm. These variables are important to evaluate when considering phage as a potential therapeutic to treat biofilm infections. Defining a controlled method of phage addition and evaluating these variables leads to optimizing these experiments in evaluating phage as a potential therapeutic agent. Studying the impact of phage size and zeta potential on biofilm penetration and optimizing phage addition methods leads to a better understanding of the potential phage has as a therapeutic agent and provides insight for future studies.

Phage Characterization

Size and Zeta Potential of Phage Andhra

Characterization of phage size and zeta potential are critical to development of phage as a biofilm therapeutic. Phage size is important as this can affect how easily the phage is able to penetrate the biofilm. Due to the EPS matrix and the porosity of the biofilm, larger particles might have more trouble penetrating the biofilm, while smaller particles can penetrate the biofilm with more ease, therefore being able to infect the bacterial cells. The zeta potential of phage is important as this impacts how the phage interact with the biofilm upon penetration. Some components of the biofilm have a negative charge, such as the bacterial cells and the proteins and extracellular DNA in the EPS matrix of the biofilm, while some components, like the PIA in the EPS matrix of the biofilm, have a positive charge (Nguyen et al., 2020; Otto, 2009). Phage charge can influence phage interactions with the various components of the biofilm.

The average diameter of phage Andhra was calculated to be 121.36 ± 1.47 nm with an average polydispersity index (PDI) of 0.3812 ± 0.0073 (Figure 14). The PDI, which determines how broad the distribution of the data is, shows that the average size of phage Andhra computed by the zetasizer is an accurate representation of the sample. A PDI under 0.5 indicates that the data computed is a good representation and provides good quality results while a PDI over 0.5 would mean inaccurate data.

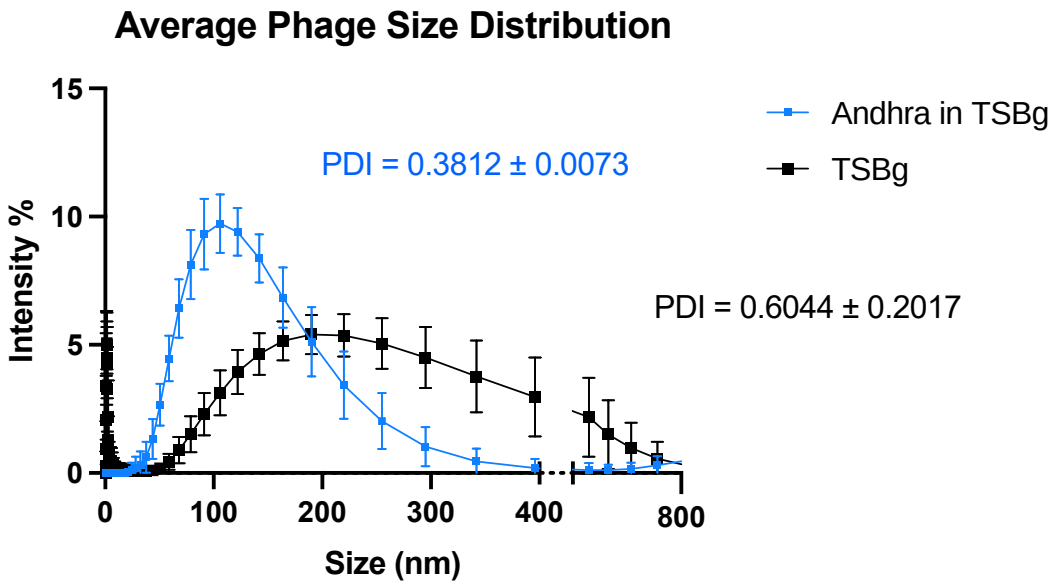

Figure 14. Phage size distribution from the different runs done on the zetasizer.

In Figure 14, the distribution of the calculated size of phage Andhra suspended in TSB_G was plotted with the distribution of TSB_G. The distribution of the control runs have a broader width that extends beyond the distribution obtained for the size of phage Andhra. There have been previous studies that have also calculated the size of phage Andhra. In one previous study, utilizing Transmission Electron Microscopy (TEM), the capsid size of phage Andhra was found to be 42.7 ± 1.5 nm in diameter (Cater et al., 2017). In another study, Electron Microscopy (EM) was used to find that the capsid size of phage Andhra was 50 nm in diameter and the tail of phage Andhra was 40 nm long (Hawkins et al., 2022). Both values calculated from these studies are lower than what I calculated as the phage size in solution. Both studies dehydrated the phage prior to EM measurements of particle size. Since I viewed the phage in a solution of TSB_G media, the size values that I calculated account for the volume occupied by the phage while they are undergoing Brownian motion. In solution, the phage particles can be oriented in any way making the volume occupied by the phage larger than what is observed in a 2D electron microscopy image. The orientation in solution is significant for particle size calculation due to the capsid and tail component of phage Andhra. Another reason that the values I calculated may be overestimating the size of phage Andhra, is that the zetasizer might be including the size calculation of other components of TSB_G. The components of TSB_G include casein, soybean meal, glucose, sodium chloride, and dipotassium phosphate. The broad distribution could be a result of the zetasizer detecting a great number of bigger particles and phage aggregating in the sample. The larger particles, which represent the components of TSB_G, are causing the larger distribution of the control in Figure 14.

Upon phage addition, the pores of the biofilm were estimated to be overall larger than the particle size of phage Andhra (Table 6). The smallest diameter (minor axis) of the pores were estimated to be 164.4 nm, which is greater than the average size of phage Andhra calculated using the zetasizer, 121.4 nm This shows that it is a possibility for the phage to exist within the pores of the biofilm without interacting with the bacterial cells or the EPS matrix of the biofilm.

Table 6. Estimated Pore Size of 24-hour Biofilms

Number of Pores	Average Total Pore Area (μm^2)	Average Pore Size (μm^2)	Average Major Axis of Pores (nm)	Average Minor Axis of Pores (nm)
1052 ± 405	420.9 ± 243.1	0.6062 ± 0.6226	253.3 ± 31.56	164.4 ± 19.23

Calculating the zeta potential of phage Andhra is significant because the charge of phage Andhra can affect how it interacts with components of the EPS matrix of the biofilm upon addition (Otto, 2009). The average zeta potential of phage Andhra was -12 ± 0.58 mV. Along with the zeta potential, the mobility and conductivity were calculated. The average mobility was -0.8172 ± 0.0389 µmcm/Vs and the average conductivity was 14.68 ± 0.3033 mS/cm (Table 7). The zeta potential measures the electrophoretic mobility of the particles, so since the average value for zeta potential was negative, phage Andhra particles are negatively charged relative to the surrounding media. The mobility measures the velocity of the particles in the solution, meaning that when the data was calculated, the particles were moving at about an average of -0.8172 µmcm/Vs. The negative in this value indicates that the particles are moving in the opposite direction of constant force. Conductivity represents the ability of the phage particles to conduct an electrical current. A higher conductivity indicates that the sample has high salt concentrations.

Table 7. Average values from calculating zeta potential

Zeta Potential (mV)	Mobility (µmcm/Vs)	Conductivity (mS/cm)
-12 ± 0.58	-0.8172 ± 0.0389	14.68 ± 0.3033

Generally, phage have a net negative zeta potential, therefore phage Andhra was expected to also have a net negative zeta potential. Other studies have utilized the zetaszier to find the zeta potential of other phage. Phage DRA88 has a zeta potential of -17 mV and phage K has a zeta potential of -26.3 mV (Alves et al., 2014). The zeta potential for phage Andhra is lower than the zeta potential of other phages. The slightly lower zeta potential could be due to the size of phage Andhra being smaller when compared to other phage. For example, phage K has an average size of 280 nm (Alves et al., 2014). Although phage have a net negative charge, upon addition to the biofilm, $CaCl_2$ is added, which neutralizes the overall charge of the phage (Chaudhry et al., 2014; Olson & Horswill, 2014). Salts within the dispersant in the sample may also affect the readings of zeta potential. The salts in TSB_G may neutralize the charge of the phage particles. If the salts in TSB_G

have a great affinity for the phage particles, the charge of the phage particles could potentially be shielded from measurement by the salts present in the dispersant (Dixon et al., 2018).

Knowing the particle size of phage Andhra allows insight as to what size the particles of phage are in comparison to the porosity of the biofilm. The net negative charge of phage Andhra is significant to know as this will make it more difficult for the phage to bind to the negatively charged components of the biofilm (Hall-Stoodley et al., 2004).

Quantitative Method for Estimating MOI Upon Phage Addition to Biofilms

To determine the MOI prior to phage treatment to biofilms, the concentrations of the phage and bacteria within the biofilm are required. This work established a quantitative method for estimating the number of bacteria within established biofilms prior to phage addition to be used for calculating MOI.

The quantitative methods for estimating the number of bacteria within the established biofilm consists of calculating the biofilm volume and local cell number density. To find the biofilm volume, the image analysis software COMSTAT was used to calculate the height and porosity of the biofilm. After setting a threshold value for the images, the height and porosity values obtained for COMSTAT were averaged from 15 different image volumes. To find the biofilm volume, the area of the well that the biofilm was grown in was multiplied by the average height and average porosity, or the proportion of the sample that is porous. The constant well area that the biofilm was grown in is $0.7\ cm^2 = 7 * 10^7 \mu m^2$. The average biofilm height and porosity (Table 8) were used to calculate the total biofilm volume, which is $8.3 * 10^8 \mu m^3$ using Equation 7 from the Methodology.

Table 8. Average values for 24-hour biofilm height and porosity calculated by COMSTAT

Average height (μm)	Average porosity	Average biomass ($\mu m^3/\mu m^2$)
23.6 ± 1.7	0.2831 ± 0.0371	17.6 ± 1.1

The number of bacterial cells and the volume of the image stack was needed to calculate the local number density of the biofilm. The number of bacterial cells were obtained using the image analysis software Trackpy (Figure 15). The average number of bacterial cells calculated from 15 different image volumes was 8641.3 bacterial cells. The image volume was calculated by multiplying the area of the image by the number of images in the stack. The image volume was calculated to be 16082.5 μm^3. Therefore, the local number density was calculated to be 0.54 $cells/\mu m^3$, using Equation 4 from the Methodology. This cell density value is greater than the

local number density of cells for an unstressed 24-hr biofilm grown in a flow-cell with a shear stress of 0.01 Pa, which was 0.19 $cells/\mu m^3$ (Stewart et al., 2013). In this paper the biofilm was grown for the same amount of time, however they grew their biofilms in flow cells, at 0.5 mL/min, instead of statically.

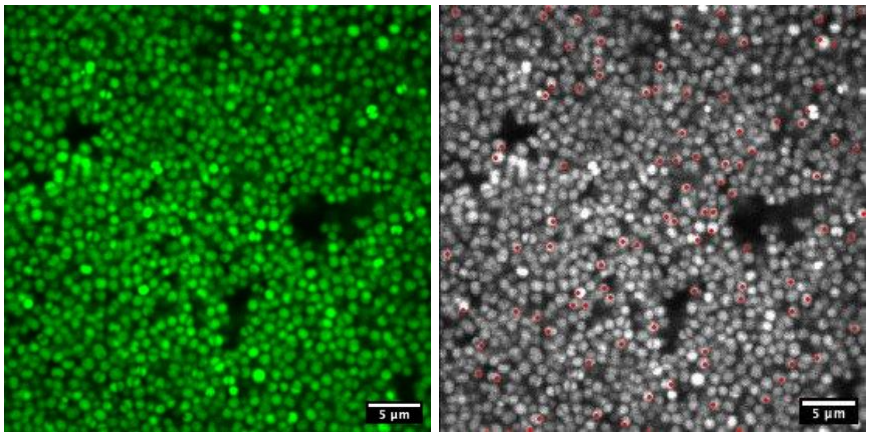

Figure 15. Trackpy Images used to Calculate Bacterial Cell Concentration.

(Left) An image near the coverslip of a 24-hr biofilm image stack. (Right) An example of an image from an image stack used by Trackpy to locate bacteria using red circle markers as identifying bacteria.

With the calculated biofilm volume and the local number density, the total number of bacterial cells in the biofilm was calculated. The total number of bacterial cells in a 24-hr biofilm was calculated to be $4.5 * 10^8$ bacterial cells.

The concentration of the phage Andhra was found using standard serial dilution methods. The highest phage concentration obtained from high titer phage lysate was $7.4 * 10^8 \pm 1.1 * 10^9$ pfu/mL.

Defining a controlled method for calculating the MOI prior to phage addition is impactful to the field of phage therapy as this allows for more reproducible experiments and accurate results. Additionally, it will enable clearer comparisons of how different phage MOIs affect the height, porosity, and biomass of the biofilm. The definitive method of calculating the MOI prior to phage treatment allows the optimization of phage Andhra concentrations to be refined.

Effect of MOI on Biofilm Growth and Structure

Before treating the biofilms with phage, I hypothesized that as MOI increases the biofilm height and biomass will decrease, while the porosity will increase. In comparison to a control 48-hour biofilm, at an MOI under 1, I hypothesized that there would be an increase in porosity near the media interface of the biofilm. At an MOI greater than 1, there will be a reduction of biofilm

biomass and increased porosity throughout the biofilm. In this study, phage-treated biofilms were analyzed at MOIs of 0 (control), 0.07, 0.67, and 1.16.

Change in Biofilm Structure of the Phage-Treated Biofilms at Different MOIs

The biofilms were treated with phage at the MOIs of 0.07, 0.67, and 1.16. I hypothesized that as MOI increases, the height and biomass will decrease. As for porosity, I hypothesized that as the MOI increases porosity will increase. I found that the height and biomass decreased at MOIs under 1, which was expected due phage lysing the bacterial cells. However, there was an increase in height and biomass between the experiments done at MOIs of 0.67 and 1.16, which was unexpected. The porosity remained consistent between the experiments done for the 24-hour biofilms (Table 8), 48-hour biofilms, and MOI = 0.07, which is expected since the growth conditions were not drastically changed for these experiments. At an MOI of 0.67, there was a 16% decrease in porosity from the MOI of 0.07, which was not expected. At an MOI of 1.16, the porosity increased, which aligned with the initial expectations that the porosity would increase when the MOI was greater than 1 (1.16). The height, porosity, and biomass of the phage treated biofilms and the control 48-hour biofilm can be seen in Table 9.

Table 9. Average Height, porosity, and biomass of 48-hour biofilms

	Average height (μm)	Average Porosity	Average Biomass ($\mu m^3/ \mu m^2$)
MOI = 0 (Control)	26.4 ± 2.4	0.2772 ± 0.0487	19.91 ± 2.74
MOI = 0.07	24.5 ± 2.6	0.2813 ± 0.0380	18.35 ± 1.89
MOI = 0.67	21.3 ± 1.8	0.2397 ± 0.0578	16.95 ± 1.36
MOI = 1.16	24.4 ± 3.0	0.3034 ± 0.0687	17.76 ± 2.99

In general, the biofilm height significantly increased from 24-hours to 48-hours in untreated biofilms (Figure 16). It is expected for the biofilm height to increase as more time is allotted for biofilm growth.

When MOI is less than 1 (0.07), biofilm height, porosity, and biomass are not significantly different than an untreated biofilm grown for 48 hours. The concentration of phage is quite low at this MOI meaning that low concentrations of MOI do not have a significant impact on the biofilm gross structure (Figure 16). Qualitative assessment of the images shows no visual difference in the porosity of the biofilm possibly due to the low concentration of phage added since porosity does not visually change when grown for an additional 24 hours. However, the height and biomass show a statistically insignificant decrease of about 8%. The slight decrease in the height and biomass at an MOI less than 1 was hypothesized. Overall, the addition of phage at an MOI less than 1 does not have a significant impact on the height, porosity, and biomass of an established biofilm.

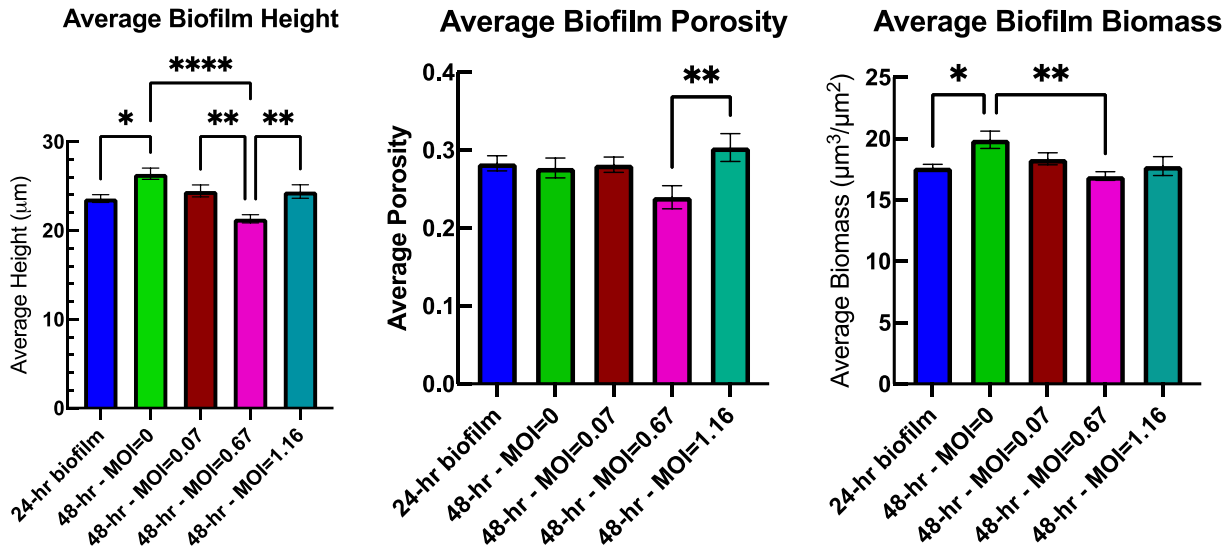

Figure 16. The average maximum height, porosity, and biomass of the control and phage-treated biofilms.

*The statistical significance indicated by * represents $p < 0.05$. Error bars are standard error of mean (SEM).*

When the MOI is slightly below 1 (0.67), the biofilm height and biomass significantly decrease, while the porosity does not significantly change, when compared to the 48-hour control. The height has a statistically significant decrease of 21%, the porosity has a statistically insignificant decrease of 16% and the biomass has a statistically significant decrease of 16% (Figure 16). Although the decrease in height is significant, the greatest difference in height seen is about 5 µm. A greater change in height would provide more concrete conclusions to be made about the effect that phage addition has on the biofilm height.

The results obtained for the height and biomass support my hypothesis that a decrease in height and biomass would occur due to increasing the phage concentration added. However, I did not expect the porosity to decrease as the phage concentration increased ten-fold. A possible reason for the decrease in porosity could be due to a phenomenon known as "lysis from without" (Abedon, 2011). This can occur when a higher concentration of phage are added to the biofilm. The abundance of viral phage particles in the biofilm may cause phage to aggregate on the surface of the bacterial cell, causing the cell membrane of the bacterial cell to rupture. This will cause the intracellular components of the host bacterial cell to disperse within the biofilm. During regular cell lysis, the phage infect and take over the bacterial host cell, causing cell death to the bacterial host cell and an increasing number of phage in the biofilm. Without the phage lysing the bacterial host cell during "lysis from without", the intracellular components of the bacterial host cell will disperse throughout the biofilm without an increase of phage particles in the biofilm. The intracellular components and the phage could then be filling in the pores throughout the biofilm.

To confirm this, an additional fluorescent dye that stains matrix material would be required to confirm the increase in intracellular components in the biofilm (Abedon, 2011; Azeredo & Sutherland, 2008).

When the MOI is greater than 1 (1.16), the height, porosity, and biomass did not significantly change when compared to the untreated 48-hour control. However, the biofilm height and porosity both significantly increased when compared to the experiment done at an MOI of 0.67. The 22% increase in porosity aligns with my hypothesis that the porosity will increase as the concentration of phage increases. There was an 18.3% increase in height between the experiments done at an MOI 0f 0.67 and 1.16 (Figure 16). The increase in height could be due to the phage becoming entrapped within the pores of the biofilm and the "lysis from without" phenomena. These scenarios can result in an increase of the biofilm height because of phage accumulation causing the intracellular components to push the bacterial cells up causing the height of the biofilm to increase.

In one study, phage treatment to established 24-hour *S. epidermidis* biofilms shows complete eradication of one of three *S. epidermidis* strains after 10 hours of incubated growth with the phage (Fanaei Pirlar et al., 2022). It is hard to follow the MOI of phage treatment in this specific paper as the MOI was only clearly reported for experiments conducted with planktonic bacteria. Another study of phage treatment to an established 48-hour *S. aureus* biofilm shows nearly a complete eradication after phage was treated for a duration of 48 additional hours. This was done at MOIs of 1 and 10. The phage added to the biofilms was a phage mixture of different phage strains. The effectiveness of this phage treatment could be due to a greater burst size of 125 pfu/cell in comparison to Andhra's burst size of 9.3 pfu/mL (Alves et al., 2014). Although it is hard to compare, greater MOIs could possibly lead to a higher reduction in biofilm biomass.

Overall, when compared to a 48-hour control biofilm, I found that the height, porosity, and biomass decreased from MOI of 0 to 0.67 and then increased when the MOI reached a value of 1.16. The average height and biomass of the biofilm decreases as the MOI increases to 0.67. For an MOI of 1.16, the height, biomass, and porosity increased. While it was predicted that the porosity would increase, the height and biomass were not expected to increase. The interactions between phage and the components of the biofilm have proven to be complex.

Conclusions and Future Work

The goal of my thesis was to analyze the effect of phage Andhra at different MOIs on the biofilm's height, porosity, and biomass. This was done by characterizing the biophysical properties of phage Andhra, developing a quantitative method for controlling MOI prior to phage treatment, and determining the effect of different phage MOIs on biofilm growth and structure.

Biophysical properties of phage Andhra were calculated. Phage Andhra particle size was found to be 121.36 nm using a zetasizer, which was larger than values found with electron microscopy. The negative zeta potential of -12 mV calculated for phage Andhra aligns with the negative zeta potentials of other phage in the literature.

A definitive method to calculate the MOI prior to phage treatment was established. This controlled method will provide a consistent way of calculating the bacterial cell concentration prior to phage addition without introducing any bias or ambiguity. The method allows for more thorough and analytical work to be done in the future.

The effect of different phage MOIs was analyzed on the biofilm height, porosity, and biomass. For MOI values below 1 (0.07, 0.67), the height and biomass of the biofilm decrease. The porosity of the biofilm increases with MOI values greater than 1. The biofilm height and biomass show a slight increase at an MOI greater than 1 (1.16) which could be due to phage aggregating within the pores of the biofilm or the "lysis from without" phenomena. The "lysis from without" phenomena could also cause a decrease in porosity at greater MOIs. These findings suggest that phage could be utilized to manipulate biofilm properties and potentially control biofilm infections.

Some limitations in this study include no experiments done at MOIs higher than 1.16. Additionally, more experiments done at each MOI would produce a lower percent error, a lower standard deviation, and provide more precise results. During the initial stage of this study there was a need to troubleshoot to accurately calculate the particle size and concentration of phage Andhra. This process took time and affected the duration for conducting additional experiments that would have helped the understanding of how various phage concentrations could affect the properties of the biofilm.

Future studies could investigate the viability of bacterial cells after phage treatment. This can be done by calculating the surface area of live cells to dead cells by using SYTO9 and Propidium Iodide (PI) stains in conjunction with sequential imaging. Different time points of phage treatment could be analyzed to observe how phage treatment affects the biofilm at the different growth stages of the biofilm. Labelling the phage fluorescently would provide insight as to how the phage that do not interact with the bacterial cells could be interacting with other biofilm components such as the EPS matrix or the pores within the biofilm. Obtaining a greater concentration of phage and fluorescently labelling the matrix materials would show whether increasing the concentration

would cause the intracellular components of the bacterial host cell to increase the biofilm biomass or if it will reduce the biofilm biomass.

The long-term impact of my work will guide future phage-biofilm studies to use this controlled method of determining the MOI prior to phage addition to accurately analyze the effect lytic phage have on the biofilm height, porosity, and biomass. This controlled method provides clarity and accuracy for any future studies that plan to compare the biofilm structure between various MOIs. This work will lead to optimizing the MOI prior to phage addition, essential for evaluating phage as a potential alternative to antibiotics.

References:

Abedon, S. T. (2011). Lysis from without. *Bacteriophage*, *1*(1), 46-49. https://doi.org/10.4161/bact.1.1.13980

Abedon, S. T., Danis-Wlodarczyk, K. M., Wozniak, D. J., & Sullivan, M. B. (2021). Improving Phage-Biofilm In Vitro Experimentation. *Viruses*, *13*(6), 1175. https://doi.org/10.3390/v13061175

Alves, D. R., Gaudion, A., Bean, J. E., Esteban, P. P., Arnot, T. C., Harper, D. R., Kot, W., Hansen, L. H., Enright, M. C., & Jenkins, A. T. A. (2014). Combined Use of Bacteriophage K and a Novel Bacteriophage To Reduce Staphylococcus aureus Biofilm Formation. *Applied and Environmental Microbiology*, *80*(21), 6694-6703. https://doi.org/doi:10.1128/AEM.01789-14

Azeredo, J., & Sutherland, I. (2008). The Use of Phages for the Removal of Infectious Biofilms. *Current Pharmaceutical Biotechnology*, *9*(4), 261-266. https://doi.org/10.2174/138920108785161604

Cater, K., Dandu, V. S., Bari, S. M., Lackey, K., Everett, G. F., & Hatoum-Aslan, A. (2017). A Novel Staphylococcus Podophage Encodes a Unique Lysin with Unusual Modular Design. *mSphere*, *2*(2). https://doi.org/10.1128/mSphere.00040-17

Cerca, N., Oliveira, R., & Azeredo, J. (2007). Susceptibility of Staphylococcus epidermidis planktonic cells and biofilms to the lytic action of staphylococcus bacteriophage K. *Lett Appl Microbiol*, *45*(3), 313-317. https://doi.org/10.1111/j.1472-765X.2007.02190.x

Chaudhry, W. N., Haq, I. U., Andleeb, S., & Qadri, I. (2014). Characterization of a virulent bacteriophage LK1 specific forCitrobacter freundiiisolated from sewage water. *Journal of Basic Microbiology*, *54*(6), 531-541. https://doi.org/10.1002/jobm.201200710

COMSTAT. www.comstat.dk

Crocker, J. C., & Grier, D. G. (1996). Methods of Digital Video Microscopy for Colloidal Studies. *Journal of Colloid and Interface Science*, *179*(1), 298-310. https://doi.org/https://doi.org/10.1006/jcis.1996.0217

Curtin, J. J., & Donlan, R. M. (2006). Using bacteriophages to reduce formation of catheter-associated biofilms by Staphylococcus epidermidis. *Antimicrob Agents Chemother*, *50*(4), 1268-1275. https://doi.org/10.1128/AAC.50.4.1268-1275.2006

Dan Allan, T. A. C., Nathan Keim, François Boulogne, Rebecca W Perry, Leonardo Uieda. (2021). *soft-matter/trackpy: Trackpy v0.5.0*. Zenodo. http://soft-matter.github.io/trackpy/v0.3.0/index.html

Dixon, M. J. L., Flint, S. H., Palmer, J. S., Love, R., Chabas, C., & Beuger, A. L. (2018). The effect of calcium on biofilm formation in dairy wastewater. *Water Practice and Technology*, *13*(2), 400-409. https://doi.org/10.2166/wpt.2018.050

Fanaei Pirlar, R., Wagemans, J., Ponce Benavente, L., Lavigne, R., Trampuz, A., & Gonzalez Moreno, M. (2022). Novel Bacteriophage Specific against Staphylococcus epidermidis and with Antibiofilm Activity. *Viruses*, *14*(6), 1340. https://doi.org/10.3390/v14061340

Gill, S. R., Fouts, D. E., Archer, G. L., Mongodin, E. F., Deboy, R. T., Ravel, J., Paulsen, I. T., Kolonay, J. F., Brinkac, L., Beanan, M., Dodson, R. J., Daugherty, S. C., Madupu, R., Angiuoli, S. V., Durkin, A. S., Haft, D. H., Vamathevan, J., Khouri, H., Utterback, T., . . . Fraser, C. M. (2005). Insights on Evolution of Virulence and Resistance from the Complete Genome Analysis of an Early Methicillin-Resistant Staphylococcus aureus Strain and a Biofilm-Producing Methicillin-Resistant Staphylococcus e.

Journal of Bacteriology, *187*(7), 2426-2438. https://doi.org/10.1128/jb.187.7.2426-2438.2005

Gutiérrez, D., Martínez, B., Rodríguez, A., & García, P. (2012). Genomic characterization of two Staphylococcus epidermidis bacteriophages with anti-biofilm potential. *BMC Genomics*, *13*(1), 228. https://doi.org/10.1186/1471-2164-13-228

Hall-Stoodley, L., Costerton, J. W., & Stoodley, P. (2004). Bacterial biofilms: from the Natural environment to infectious diseases. *Nature Reviews Microbiology*, *2*(2), 95-108. https://doi.org/10.1038/nrmicro821

Hansen, M. F., Svenningsen, S. L., Røder, H. L., Middelboe, M., & Burmølle, M. (2019). Big Impact of the Tiny: Bacteriophage–Bacteria Interactions in Biofilms. *Trends in Microbiology*, *27*(9), 739-752. https://doi.org/https://doi.org/10.1016/j.tim.2019.04.006

Hatoum-Aslan, A. (2021). The phages of staphylococci: critical catalysts in health and disease. *Trends in Microbiology*, *29*(12), 1117-1129. https://doi.org/https://doi.org/10.1016/j.tim.2021.04.008

Hawkins, N. T. C., Kizziah, J. L., Hatoum-Aslan, A., & Dokland, T. (2022). *Structure and host specificity of Staphylococcus epidermidis bacteriophage Andhra*. Cold Spring Harbor Laboratory. https://dx.doi.org/10.1101/2022.07.21.500982

Henriksen, K., Rørbo, N., Rybtke, Morten L., Martinet, Mark G., Tolker-Nielsen, T., Høiby, N., Middelboe, M., & Ciofu, O. (2019). P. aeruginosa flow-cell biofilms are enhanced by repeated phage treatments but can be eradicated by phage–ciprofloxacin combination: — monitoring the phage–P. aeruginosa biofilms interactions. *Pathogens and Disease*, *77*(2). https://doi.org/10.1093/femspd/ftz011

Heydorn, A., Nielsen, A. T., Hentzer, M., Sternberg, C., Givskov, M., Ersbøll, B. K., & Molin, S. (2000). Quantification of biofilm structures by the novel computer program comstat. *Microbiology*, *146*(10), 2395-2407. https://doi.org/10.1099/00221287-146-10-2395

Hobbs, Z., & Abedon, S. T. (2016). Diversity of phage infection types and associated terminology: the problem with 'Lytic or lysogenic'. *FEMS microbiology letters*, *363*(7).

Kao, P.-K., Solomon, M., & Ganesan, M. (2021). *Shape anisotropy enhances the elasticity of colloidal gels through mechanisms that act multiplicatively*.

Lacqua, A., Wanner, O., Colangelo, T., Martinotti, M. G., & Landini, P. (2006). Emergence of Biofilm-Forming Subpopulations upon Exposure of Escherichia coli to Environmental Bacteriophages. *Applied and Environmental Microbiology*, *72*(1), 956-959. https://doi.org/doi:10.1128/AEM.72.1.956-959.2006

Lungren, M. P., Christensen, D., Kankotia, R., Falk, I., Paxton, B. E., & Kim, C. Y. (2013). Bacteriophage K for reduction ofStaphylococcus aureusbiofilm on central venous catheter material. *Bacteriophage*, *3*(4), e26825. https://doi.org/10.4161/bact.26825

Malvern. (2013). Zetasizer. In M. I. Ltd (Ed.), (1.1 ed., pp. 74-76). Enigma Business Park, Grovewood Road, Worcestershire WR14 1XZ United Kingdom.

Marianne Poxleitner, W. P., Deborah Jacobs-Sera, Viknesh Sivanathan, Graham Hatfull. (2018). *Phage Discovery Guide* https://seaphagesphagediscoveryguide.helpdocsonline.com/home

Nguyen, H. T. T., Nguyen, T. H., & Otto, M. (2020). The staphylococcal exopolysaccharide PIA - Biosynthesis and role in biofilm formation, colonization, and infection. *Comput Struct Biotechnol J*, *18*, 3324-3334. https://doi.org/10.1016/j.csbj.2020.10.027

Olson, M. E., & Horswill, A. R. (2014). Bacteriophage Transduction in Staphylococcus epidermidis. In (pp. 167-172). Humana Press. https://doi.org/10.1007/978-1-62703-736-5_15

Otto, M. (2009). Staphylococcus epidermidis — the 'accidental' pathogen. *Nature Reviews Microbiology*, *7*(8), 555-567. https://doi.org/10.1038/nrmicro2182

Shabram, P., & Aguilar-Cordova, E. (2000). Multiplicity of Infection/Multiplicity of Confusion. *Molecular Therapy*, *2*(5), 420-421. https://doi.org/10.1006/mthe.2000.0212

Stewart, E. J., Satorius, A. E., Younger, J. G., & Solomon, M. J. (2013). Role of Environmental and Antibiotic Stress on Staphylococcus epidermidis Biofilm Microstructure. *Langmuir*, *29*(23), 7017-7024. https://doi.org/10.1021/la401322k

Vidakovic, L., Singh, P. K., Hartmann, R., Nadell, C. D., & Drescher, K. (2018). Dynamic biofilm architecture confers individual and collective mechanisms of viral protection. *Nature Microbiology*, *3*(1), 26-31. https://doi.org/10.1038/s41564-017-0050-1

Vorregaard, M. (2008). *Comstat2 - a modern 3D image analysis environment for biofilms in Informatics and Mathematical Modeling, Technical University of Denmark: Kongens Lyngby, Denmark.*

Xu, L. C., & Siedlecki, C. A. (2022). Submicron topography design for controlling staphylococcal bacterial adhesion and biofilm formation. *Journal of Biomedical Materials Research Part A*, *110*(6), 1238-1250. https://doi.org/10.1002/jbm.a.37369